Biochemistry

Article

Cite This: *Biochemistry* 2019, 58, 1363−1378

pubs.acs.org/biochemistry

Transition-State Interactions in a Promiscuous Enzyme: Sulfate and Phosphate Monoester Hydrolysis by *Pseudomonas aeruginosa* Arylsulfatase

Bert van Loo,[†,§] Ryan Berry,[‡] Usa Boonyuen,[†,∥] Mark F. Mohamed,[†] Marko Golicnik,[†,⊥] Alvan C. Hengge,[*,‡] and Florian Hollfelder[*,†]

[†]Department of Biochemistry, University of Cambridge, Cambridge, United Kingdom

[‡]Department of Chemistry and Biochemistry, Utah State University, Logan, Utah 84322, United States

Supporting Information

ABSTRACT: *Pseudomonas aeruginosa* arylsulfatase (PAS) hydrolyzes sulfate and, promiscuously, phosphate monoesters. Enzyme-catalyzed sulfate transfer is crucial to a wide variety of biological processes, but detailed studies of the mechanistic contributions to its catalysis are lacking. We present linear free energy relationships (LFERs) and kinetic isotope effects (KIEs) of PAS and analyses of active site mutants that suggest a key role for leaving group (LG) stabilization. In LFERs PAS^{WT} has a much less negative Brønsted coefficient ($\beta_{lg}^{obs\text{-}Enz} = -0.33$) than the uncatalyzed reaction ($\beta_{lg}^{obs} = -1.81$). This situation is diminished when cationic active site groups are exchanged for alanine. The considerable degree of bond breaking during the transition state (TS) is evidenced by an $^{18}O_{bridge}$ KIE of 1.0088. LFER and KIE data for several active site mutants point to leaving group stabilization by active site K375, in cooperation with H211. ^{15}N KIEs and the increased sensitivity to leaving group ability of the sulfatase activity in neat D_2O ($\Delta\beta_{lg}^{H\text{-}D} = +0.06$) suggest that the mechanism for S−O_{bridge} bond fission shifts, with decreasing leaving group ability, from charge compensation via Lewis acid interactions toward direct proton donation. $^{18}O_{nonbridge}$ KIEs indicate that the TS for PAS-catalyzed sulfate monoester hydrolysis has a significantly more associative character compared to the uncatalyzed reaction, while PAS-catalyzed phosphate monoester hydrolysis does not show this shift. This difference in enzyme-catalyzed TSs appears to be the major factor favoring specificity toward sulfate over phosphate esters by this promiscuous hydrolase, since other features are either too similar (uncatalyzed TS) or inherently favor phosphate (charge).

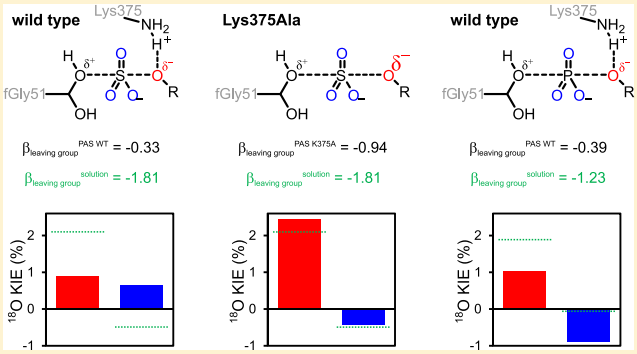

Arylsulfatases catalyze the *in vivo* hydrolysis of sulfate monoesters, producing inorganic sulfate, typically removing it from a sugar or a steroid hormone. Sulfatases are highly proficient enzymes, with catalytic proficiencies ($(k_{cat}/K_M)/k_{uncat}$) well above 1×10^{13} to 1×10^{17} M^{-1} for the model substrate 4-nitrophenyl sulfate **1d** (Scheme 1).[1−4] Despite their occurrence in eukaryotes and prokaryotes, relevance for a variety of key processes (e.g., development,[5−11] germination,[12] resistance against toxic defense molecules,[13,14] mucin desulfatation,[15−17] or degradation of mucopolysaccharides[18,19]) and the danger of various diseases as a result of their malfunction (e.g., lysosomal disorders[18,20]), their mechanism has not been studied in the same detail as that of the related phosphatases.

Scheme 1. General Reaction Scheme for the PAS-Catalyzed Hydrolysis of Aryl Sulfate Monoesters 1a−1l and Aryl Phosphate Monoesters 2b−2l

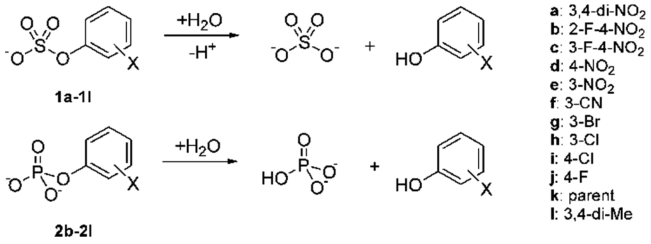

The majority of sulfatases known are members of the alkaline phosphatase (AP) superfamily. The mechanism of transition state (TS) stabilization during enzyme-catalyzed substrate hydrolysis of one member of this superfamily, *Escherichia coli* alkaline phosphatase (*Ec*AP), has been subject of a large number of in-depth studies involving the experimental tools of linear free energy relationships (LFERs), kinetic isotope effects (KIEs), mutant studies, and structural analysis by X-ray crystallog-

Received: September 18, 2018
Revised: January 11, 2019
Published: February 27, 2019

DOI: 10.1021/acs.biochem.8b00996
Biochemistry 2019, 58, 1363−1378

raphy.[21−37] In addition computational simulations have been employed to pinpoint transition-state interactions.[27,28,38−43]

Sulfatase members of the AP superfamily have been studied less extensively. Catalytically important residues have been shown to be conserved among the arylsulfatases[2,4,44−48] and mutant studies (e.g., of human arylsulfatase A,[49] choline sulfatase,[4] and the closely related phosphonate monoester hydrolase[50]) have suggested that many of these conserved residues are indeed involved in the catalytic pathway in the enzyme active site. LFERs and KIEs have been measured for a number of phosphatases,[21−24,36,51−59] but only one such study is available for sulfatases.[60]

In addition to the family relationship, members of the AP superfamily are also typically catalytically promiscuous;[61−63] that is, they catalyze multiple, chemically distinct reactions with large rate accelerations.[64,65] Within the superfamily reciprocal relationships of crosswise catalytic promiscuity are observed; that is, the promiscuous activity of one member is the native function of another, and *vice versa*.[64,65] Given the postulated role of promiscuity in evolution by gene duplication,[61,66] functional crossover defines such functional relationships as pathways for respecialization or repurposing in enzyme superfamilies,[67] which was experimentally demonstrated recently by a more than 10^7-fold specificity switch of a sulfatase to enhance phosphonate hydrolase activity.[68] As catalysis for the activity under selective pressure must be maintained at a relevant level during evolution, the question of how mechanistic features of these enzymes can be effective for catalysis of different reactions arises.

In this work we studied the reactions catalyzed by the promiscuous arylsulfatase from *Pseudomonas aeruginosa* (PAS) using LFERs and KIEs. PAS has a wide active site opening[44] and—in contrast to sulfatases with high specificity for a particular leaving group (such as a sugar moiety[69,70] or choline[4])—accepts a range of aromatic substrates: so that the construction of LFERs based on series of aryl sulfates of different reactivity is possible with minimal interference from unique binding effects. PAS operates at high rates ($k_{cat}/K_M = 4.9 \times 10^7$ s^{-1} M^{-1}), even for the hydrolysis of the non-natural substrate 4-nitrophenyl sulfate **1d**.[1] In addition, PAS promiscuously catalyzes the hydrolyses of phosphate mono-[1] and diesters[63] as well as phosphonates,[71] thus covering mechanistically distinct hydrolase reactions.[72] However, despite its catalytic promiscuity, PAS is a genuine sulfatase: it is typically expressed under sulfate starvation conditions, part of an operon coding for sulfate-processing enzymes, and thought to act as a sulfate scavenger.[73,74]

On the basis of the X-ray structure of PAS[44] (and those of the human arylsulfatases A[47,75] (hASA) and B[45] (hASB) combined with mutant data for hASA[49]) a double displacement catalytic pathway was proposed, in which a post-translationally modified cysteine,[76] formylglycine fGly51, performs a nucleophilic attack on the sulfur center (Figure 1b). The covalent hemiacetal intermediate is broken down with assistance of H115 acting as a general base (step 2 in Figure 1b). Finally the aldehyde form of the fGly nucleophile is again hydrated, regenerating the enzyme for the next round of catalysis. Mutant data for several of the analogous active site residues in hASA show that a single mutation of one of the residues likely to be involved in charge compensation during the TS results in lowered but still detectable levels of activity.[49] During the hydrolysis of sulfates, negative charge is expected to build up in the TS on the sulfuryl group and on the leaving group.[3,77] TS stabilization can be

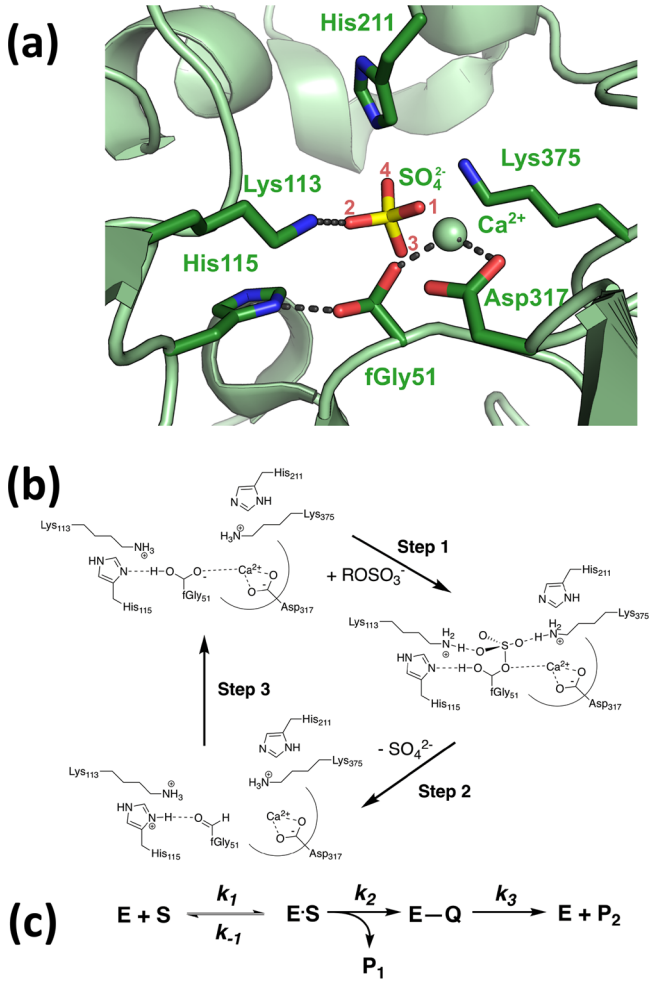

Figure 1. Active site and reaction mechanism of PAS. (**a**) 3D representation of the active site of PAS with a bound sulfate ion.[44] The assignment of the analogous nonbridging (O_1−O_3) and bridging (O_4) oxygens in the sulfate ester substrate were based on positions of the active site residues in the X-ray structure of human arylsulfatase A C69A[75] with *p*-nitrocatechol sulfate bound in the active site. (**b**) Proposed catalytic pathway for PAS-catalyzed sulfate monoester hydrolysis. When the sulfate monoester substrate is bound, the hydrated fGly51 performs a nucleophilic attack on the sulfur atom, and the bond to the alcohol leaving group (ROH) is broken (S−O_{bridge} bond fission) (step 1). The covalent intermediate is broken down by base-catalyzed hemiacetal cleavage in which inorganic sulfate acts as the leaving group (step 2). The enzyme is subsequently regenerated by hydration of the formylglycine aldehyde (step 3). (**c**) Schematic representation of the steps in (b). k_1 is the rate of formation of the enzyme−substrate (ES) complex from free enzyme (E) and substrate (S), and k_{-1} represents the dissociation rate of the ES complex. k_2 is the rate constant for the nucleophilic attack of the hydrated formylglycine and subsequent S−O_{bridge} bond fission (step 1), and k_3 is that of hemiacetal cleavage (step 2). The rehydration of the fGly residue (step 3) is expected to be several orders faster that hemiacetal cleavage and thus was not considered for the interpretation of pre-steady-state kinetics. Product P_1 is the phenolate leaving group expelled from the substrate in step 1; product P_2 is inorganic sulfate.

achieved by offsetting this charge build-up: using positively charged functionalities such as metal ions or by using hydrogen bonding or electrostatic interaction with positively charged amino acid side chains. The latter possibly may involve proton transfer to the leaving-group oxygen. The active site of PAS contains a number of residues that could neutralize charge build-

DOI: 10.1021/acs.biochem.8b00996
Biochemistry 2019, 58, 1363−1378

up on oxygen atoms during the transition state or affect the pK_a of the formylglycine (fGly51) nucleophile (Figure 1).

Here we provide a detailed quantitative examination of the interaction of active site residues with the TS in the arylsulfatase-catalyzed reaction. We use LFER and KIE data to compare the nature of the TS for the native PAS-catalyzed sulfate monoester hydrolysis with the uncatalyzed reaction and show that, while both are dissociative, the TS of the enzyme-catalyzed reaction has somewhat more associative character. The latter difference is absent for phosphate monoester hydrolysis. Finally, changes in LFERs and KIEs as a result of alanine scanning mutagenesis of PAS active site residues suggest that K375 serves as the general acid that minimizes leaving group charge change in the TS and provides leaving group stabilization.

MATERIALS AND METHODS

Sulfate Monoester Compounds for Linear Free Energy Relationships and Kinetic Isotope Effect Studies. Sulfate monoester **1d** and phosphate monoesters **2d** and **2k** (Scheme 1) were purchased from Sigma. Sulfate esters were synthesized from the respective phenol and chlorosulfonic acid; phosphate monoesters were synthesized from phosphoryl chloride and the respective phenol. Detailed procedures are given in the Supporting Information. The isotopically labeled forms of 4-nitrophenyl sulfate (**1d**)[78] and phosphate (**2d**)[53] for measurement of kinetic isotope effects were synthesized as described previously.

Protein Production and Purification. Expression of recombinant *Pseudomonas aeruginosa* Arylsulfatase (PAS, Uniprot ID K9NCQ5) from plasmid pME4322[79] and derived mutants was done in *E. coli* BL21 (DE3) growing in lysogeny broth (LB) or yeast−trypton medium (2YT) containing 30 mg mL^{-1} kanamycin. The cells were grown at 37 °C, until an OD_{600} of ∼0.6−0.8 was reached. The culture was cooled to 30 (WT) or 20 °C (mutants), isopropyl β-D-1-thiogalactopyranoside (IPTG) was added up to 0.75 mM, and the culture was grown for 4 h at 30 °C (WT) or overnight at 20 °C (mutants).

Cells expressing PAS were harvested by centrifugation and resuspended in 50 mM tris(hydroxymethyl)aminomethane (Tris) HCl pH 8.0. One tablet of complete ethylenediaminetetraacetic acid (EDTA)-free protease inhibitor cocktail (Roche) per 12 g of wet cell pellet was added to the suspension, and the cells were lysed either by using an emulsiflex-C5 homogenizer (Avestin) or by sonication. Cell-free extract (CFE) was obtained by centrifugation of the crude cell lysate at 30 000*g* for 90 min. The PAS variants were purified from CFE by subsequent anion exchange (Q-sepharose), hydrophobic interaction (phenyl sepharose), and size exclusion (Superdex 200) chromatography. All steps were performed in 50 mM Tris-HCl pH 8.0 with the appropriate additive for each step. The anion exchange chromatography was performed as described before.[1] Protein-containing fractions that eluted from the anion exchange column were pooled, and the combined fractions were brought to 200 mM $(NH_4)_2SO_4$ by adding the appropriate volume of 50 mM Tris-HCl pH 8.0 + 2 M $(NH_4)_2SO_4$ and subsequently loaded onto a phenyl sepharose hydrophobic interaction column. The column was washed with two column volumes (CV) of 50 mM Tris-HCl pH 8.0 + 200 mM $(NH_4)_2SO_4$. Protein was eluted from the column with a gradient of 200−0 mM $(NH_4)_2SO_4$ in 50 mM Tris-HCl over five CV followed by a further five CV with 50 mM Tris-HCl pH 8.0. Fractions containing active protein were pooled and concentrated into 50 mM Tris-HCl pH 8.0 to ∼10−15 mg mL^{-1} protein. The concentrated protein was loaded onto a Superdex 200 prep grade gel filtration column. PAS eluted at the expected elution volume of monomeric PAS. Protein-containing fractions were pooled and concentrated to 100−350 μM in 50 mM Tris-HCl and aliquoted in appropriate portions, flash frozen in liquid N_2, and stored at −20 °C. Protein concentrations were calculated based on the molar extinction coefficient at λ = 280 nm, ε_{280} = 102 790 M^{-1} cm^{-1}, calculated from the amino acid sequences using ProtParam (http://expasy.org/tools/protparam.html).

Construction of Mutants. All mutants of PAS, except for mutant C51S, which was constructed previously,[1] were made by site-directed mutagenesis according to the QuikChange protocol (Agilent), using primers listed in Table S16, Supporting Information and the appropriate template plasmid.

Enzyme Kinetics. All data for steady-state enzyme kinetics were recorded at 25 °C in 100 mM Tris-HCl pH 8.0 supplemented with 500 mM NaCl or as indicated. Observed initial rates (V_{obs}) were determined by following an increase in absorbance at a fixed wavelength (ranging from 270 to 400 nm depending on the substrate) as a result of product formation over time in microtiterplates (Spectramax Plus, Molecular Devices) or quartz cuvettes (Varian 100 Bio). Catalytic parameters k_{cat}, K_M, and/or k_{cat}/K_M were obtained by fitting the dependency of V_{obs} on substrate concentration ([S]) at a fixed enzyme concentration ([Enz]) (eq 1).

$$V_{obs} = \frac{k_{cat} \times [Enz] \times [S]}{K_M + [S]} \quad (1)$$

The dependency of the various kinetic parameters (k_{cat}, $1/K_M$, and k_{cat}/K_M, represented by K in eq 2) on leaving group ability (as represented by their pK_a value) was fitted to eq 2 to obtain the observed Brønsted constants for leaving group dependence ($\beta_{leaving\ group}^{obs}$).

$$\log[K] = \beta_{leavinggroup}^{obs} \times pK_a^{leavinggroup} + C \quad (2)$$

Stopped-Flow Kinetics. Fast kinetics for PAS WT-catalyzed hydrolysis of sulfate monoester **1d** were recorded using a SX20 stopped-flow setup (Applied Photophysics). No unambiguous burst phase could be detected with PAS concentrations between 1 and 8 μM and 1 mM sulfate monoester **1d**, with 100 mM Tris-HCl pH 8.0, containing 500 mM NaCl at 20 °C. Data are shown in Figure S3.

Kinetic Isotope Effects (KIEs). Natural abundance **1d** or **2d** was used for measurements of $^{15}(V/K)$. The ^{18}O KIEs $^{18}(V/K)_{bridge}$ and $^{18}(V/K)_{nonbridge}$ were measured by the remote label method, using the nitrogen atom in *p*-nitrophenol as a reporter for isotopic fractionation in labeled bridging or nonbridging oxygen positions.[80] The particular isotopic isomers used are shown in the Supporting Information. Isotope effect experiments used 100 μmol of substrate, at 25 °C in 50 mM Tris buffer, pH 8.0. The substrate concentration was 19 mM, and the reactions were started by addition of wild-type or mutant enzyme, 1 μM for substrate **1d**, and 725 μM for substrate **2d**. After reactions reached completion levels between 40% and 60% they were stopped by titration to pH 3 with HCl. Protocols for isolation of *p*-nitrophenol, isotopic analysis, and calculation of the isotope effects were the same as previously described,[53,78] and they are described in the Supporting Information.

RESULTS AND DISCUSSION

Determination and Interpretation of Steady-State Parameters. Purified PAS WT[1] was used to determine

DOI: 10.1021/acs.biochem.8b00996
Biochemistry 2019, 58, 1363−1378

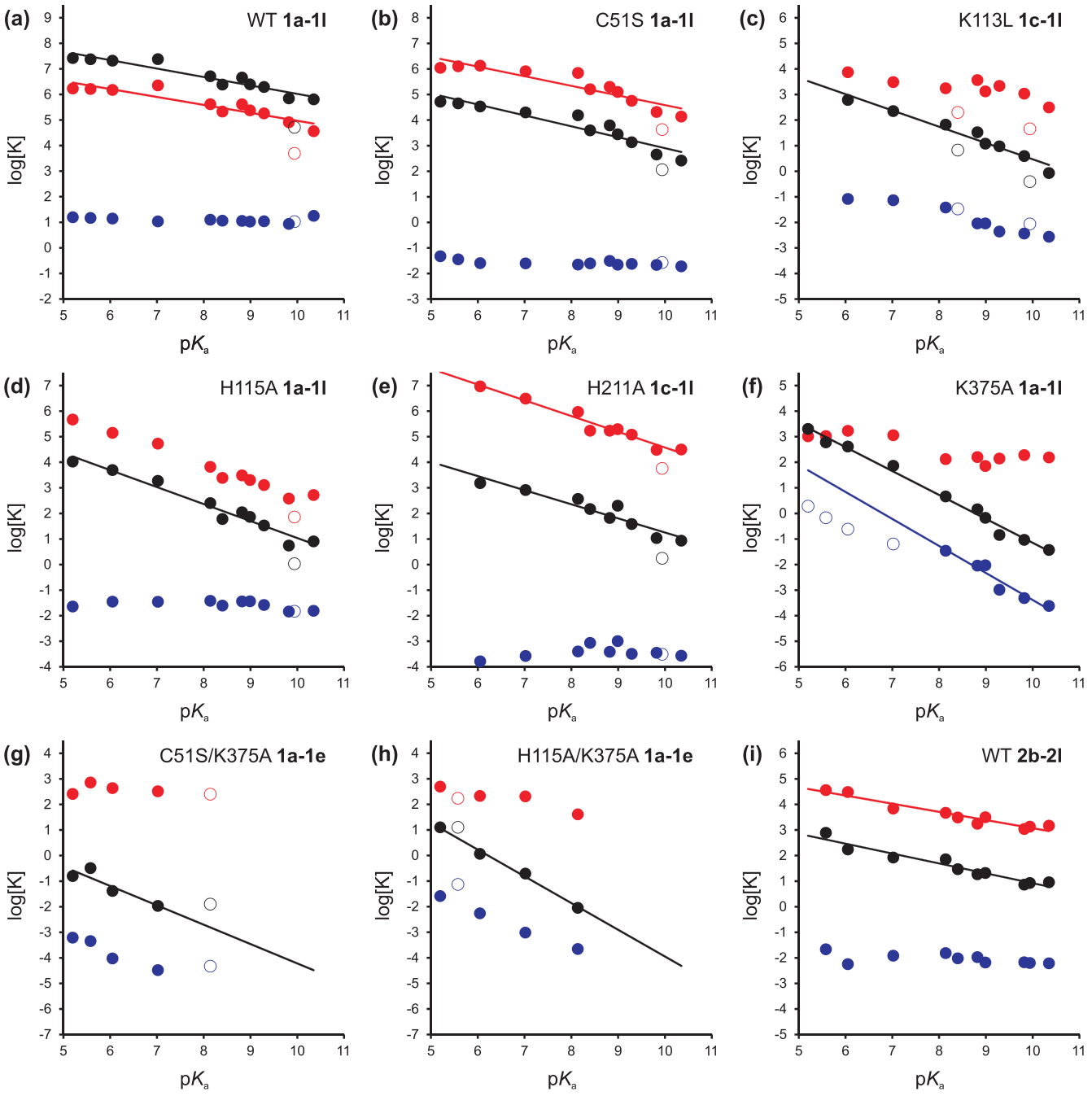

Figure 2. Dependence of catalytic parameters k_{cat} (blue) $1/K_M$ (red) and k_{cat}/K_M (black) (log values) for PAS-catalyzed hydrolysis of sulfate monoesters on leaving group ability (as represented by the pK_a of the free phenol in solution). (**a**) PAS WT (see for a superposition of the data measured here with that of Williams et al.[60] in Figure S6, Supporting Information); (**b**) PAS C51S; (**c**) PAS K113L; (**d**) PAS H115A; (**e**) PAS H211A; (**f**) PAS K375A; (**g**) PAS C51S/K375A; (**h**) PAS H115A/K375A; (**i**) PAS WT with phosphate monoesters. All data were obtained in 100 mM Tris-HCl pH 8.0; 500 mM NaCl at 25 °C. The resulting slopes ($=\beta_{leaving\ group}^{obs}$) are listed in Tables 1 and S14. The data for the unsubstituted phenol sulfate monoester **1k** deviated significantly from the trend for all enzymes, suggesting a consistent unique difference in binding compared to the other sulfate monoester substrates and were therefore not included in any of the fits. Data points represented by open circles were not included in the fits: e.g., **1f** in panel (c), in which the fitted value for K_M deviated by an order of magnitude; **1a**−**1d** in panel (f) for the fit in blue, where the slope for k_{cat} was only expected to be relevant for the TS if fully representing the rate-limiting step: this is only the case for leaving groups with pK_a > 8, so other points were excluded to reflect the chemical reaction in $\beta_{leaving\ group}^{obs}$ as much as possible; see also Figure S10, Supporting Information; **1e** in panel (g) and **1b** in panel (h) were excluded, because one parameter deviated strongly, again suggesting idiosyncratic effects in these substrates. All data for the kinetic parameters are listed in the Supporting Information (Tables S1 and S3−S10).

Michaelis−Menten parameters k_{cat}, K_M, and k_{cat}/K_M for a series of phenyl sulfate monoesters (compounds **1a**−**1l**, Scheme 1) with varying leaving group abilities (represented by their pK_a values, which range from 5.2 to 10.35 (Table S1 and Figures S1 and S2, Supporting Information). These substrates provide insight into the nature of the TS of PAS-catalyzed sulfate monoester hydrolysis by allowing the construction of LFERs,

DOI: 10.1021/acs.biochem.8b00996
Biochemistry 2019, 58, 1363−1378

similar to those reported for several phosphoryl transfer enzymes.[22,23,32,33,56−59,72,81,105]

The underlying meaning of the steady-state parameters used to monitor the bond-making and -breaking processes must be carefully considered. Since the steady-state catalytic rate constant (k_{cat}) was shown to be essentially independent of leaving group ability (Figure 2a, varying between 9 and 18 s^{-1}, Table S1, Supporting Information), it does not reflect the substrate reactivity. On the basis of the kinetic scheme for enzyme-catalyzed substrate hydrolysis (Figure 1c), the relevant rate constant to probe the nature of the TS should be k_2. If enzyme-catalyzed cleavage of the sulfate ester bond were fully rate-limiting, the steady-state catalytic rate constant k_{cat} would be essentially equal to k_2 (equation S14, Supporting Information). If this is not the case, that is, if $k_2 \geq k_3$, more complex terms arise (see equations S1−3, Supporting Information). Assuming that the substrate binding constants ($K_D = k_{-1}/k_1$) are similar for the complete series of sulfate monoesters (Scheme 1), k_{cat}/K_M reports on all steps from free enzyme and substrate to the first irreversible transition state. In this case the formation of the covalent intermediate between the formylglycine nucleophile and the respective sulfur center of the substrates that leads to leaving group departure is likely to be irreversible, as no significant inhibition by the phenolate product is observed (see equations S1−S3 in the Supporting Information for details on the relation between the Michaelis−Menten parameters and the individual rate constants for the various enzymatic steps).

LFER for PAS WT-Catalyzed Sulfate Monoester Hydrolysis. Plots of k_{cat}/K_M against the leaving group pK_a (Figure 2) were linear, with a $\beta_{leaving\ group}^{obs}$ of −0.33 (Table 1) that was considerably less negative than that of the rate for the uncatalyzed hydrolysis reaction (k_{uncat}), for which a $\beta_{leaving\ group}^{obs}$ of −1.81 has been measured.[3] This work partially reproduces a study of Williams *et al.*,[60] who recently constructed an LFER for PAS but arrived at a much steeper slope (−0.86). A comparison of both studies (see Figure S6, Supporting Information) shows that most points superimpose well with our data but that the following factors seem to have resulted in a distortion of the slope due to idiosyncratic effects of substrates (e.g., due to steric clashes or interactions between active site residues and phenolate substituents): (i) the choice of leaving groups with higher pK_a (specifically the inclusion of the bulky 4-amino-acetyl- and 4-methoxyphenolate), (ii) the narrower range of pK_a values (three compared to almost five log units covered here) and (iii) basing the study on overall fewer data points (7 *vs* 12 in our work) with worse significance (*p*-value, 0.026 vs less than 1×10^{-4}) and correlation coefficients (R^2, 0.66 vs 0.91). Starting from the quantitatively different values for $\beta_{leaving\ group}^{obs}$ our analysis below naturally differs from that of Williams et al. However, the slope $\beta_{leaving\ group}^{obs}$, is *less* steep compared to that for the solution reaction in both studies, despite the quantitative differences.

Table 1. Overview of the Observed Brønsted Constants for Leaving Group Dependence ($\beta_{leaving\ group}^{obs}$) of k_{cat}/K_M for PAS-Catalyzed Sulfate and Phosphate Monoester Hydrolysis[a]

reaction	catalyst	$\beta_{leaving\ group}^{obs}$
sulfate monoesters	solution (neutral)	−0.27[b]
	solution (monoanion)	−1.81[b]
	WT	−0.33 ± 0.04
	C51S	−0.43 ± 0.05
	K113L	−0.64 ± 0.06
	H115A	−0.67 ± 0.05
	H211A	−0.55 ± 0.07
	K375A	−0.94 ± 0.04
	C51S/K375A	−0.76 ± 0.24
	K113L/K375A	nd[c]
	H115A/K375A	−1.04 ± 0.06
	H211A/K375A	nd[c]
phosphate monoesters	solution (monoanion)	−0.27[d]
	solution (dianion)	−1.23[d]
	WT	−0.39 ± 0.04

[a]All enzymatic reactions performed in 100 mM Tris-HCl pH 8.0, 500 mM NaCl, 25 °C. [b]Edwards et al.,[3] H_2O as the nucleophile. [c]Not determined. Activity too low to be detectable. [d]Kirby & Varvoglis,[82] H_2O as the nucleophile.

A possible cause for the considerably less negative $\beta_{leaving\ group}^{obs}$ compared to the solution reaction could be that the k_{cat}/K_M values do not only represent a chemical step, as shown previously for wild-type *E. coli* alkaline phosphatase (*Ec*AP).[35,53,83] However, considerations summarized in the Supporting Information (section H) rule out diffusion control and suggest that the deviation of $\beta_{leaving\ group}^{obs}$ from the $\beta_{leaving\ group}$ of the solution reaction is a genuine effect of substrate binding and turnover by the enzyme.

Previous experimental studies into the nature of the TS of enzyme-catalyzed sulfate transfer using LFERs[60,84] typically showed less steep correlations than the corresponding solution reaction,[85−88] bringing the Brønsted slopes to values closer to zero. This decrease could be ascribed to interactions with cationic groups in the active site, but no KIEs or mutational data were available to check this hypothesis. In addition an LFER for sulfate transfer has been reported for the promiscuous sulfatase activity of AP WT.[31] Subsequent KIE studies showed that in this case a dissociative TS is likely.[21] In AP the less negative $\beta_{leaving\ group}^{obs}$ compared to the solution reaction could arise from interaction of the leaving group with positively charged moieties in the enzyme active site, most likely a divalent metal ion (Zn^{2+}). The latter phenomenon has also been reported for AP-catalyzed phosphate monoester hydrolysis.[89] In several protein tyrosine phosphatases a protonated aspartate was identified as responsible for leaving group stabilization.[51,52,54−56,59] Replacement of this aspartate with asparagine restored the leaving group dependence to a value close to that of the solution reaction.[56] In protein phosphatase 1 (PP1), a histidine was proposed to assume the same role, although practical limitations (low yield and poor activity) prevented experimental verification.[58]

LFER for PAS WT-Catalyzed Phosphate Monoester Hydrolysis. The fact that PAS WT is also a proficient phosphatase[1] ($(k_{cat}/K_M)/k_{uncat} = 2.9 \times 10^{11}$ M^{-1} toward phosphate monoester **2d**) opens the possibility of studying two reactions that proceed through similar TSs in solution[31,53,77,82,90,91] in a single active site and also facilitates comparisons with the more widely studied phosphatases.

Michaelis−Menten parameters were determined for a series of phosphate monoesters (**2b−2l**, Scheme 1). As for the sulfatase reaction, k_{cat} is practically independent of the leaving group pK_a (varying between 0.6 and 1.2×10^{-2} s^{-1}, Figure 2i and Table S3, Supporting Information), suggesting that the rate-limiting step for phosphate as well as sulfate monoesters is not leaving group-dependent. The K_M values increase with leaving group pK_a and range from 0.03 to 0.92 mM, ca. 100-fold higher

DOI: 10.1021/acs.biochem.8b00996
Biochemistry 2019, 58, 1363−1378

than for sulfatase activity. The slope of the Brønsted plot $\beta_{leaving\ group}^{obs}$ for k_{cat}/K_M for phosphate monoester hydrolysis is -0.39 ± 0.04 (Table 1), identical within the error margins to the value observed for the sulfatase reaction (and confirmed by a cross-correlation graph with a slope of unity; see Figure S9, Supporting Information). As observed for the sulfatase reaction, enzyme-catalyzed phosphate monoester hydrolysis is considerably less sensitive to leaving group ability than the solution reaction for the phosphate monoester dianion ($\beta_{leaving\ group} = -1.23$[82]). As for sulfate monoester hydrolysis, these considerable deviations can be caused by stabilization/masking of locally developing negative charge, in particular, on the leaving group oxygen. This idea is probed in the next paragraph. The less negative value for $\beta_{leaving\ group}$ is also consistent with an intrinsically more associative nature of the respective enzymatic TSs (compared to the solution reaction), possibly reinforced by the presence of cationic groups in the active site. This interpretation assumes the same degree of nucleophilic involvement. If this is not the case, the $\beta_{leaving\ group}$ value will only reflect the extent of leaving group cleavage. However, kinetic isotope effect studies (see below for details) discounted these possibilities and suggested that the TS is similar (but not identical) to the solution reaction, as in previously studied phosphatases.[23,37,56,58,59]

The Effect of Mutations on the $\beta_{leaving\ group}^{obs}$ for Sulfate Monoester Hydrolysis. As discussed above, the $\beta_{leaving\ group}^{obs}$ of enzyme-catalyzed phosphate and sulfate transfer reactions can be influenced by compensation by positively charged moieties in the active site of the negative charge build-up that occurs during the TS.[23,33,37,58,84] Furthermore the change in nucleophile between the solution (H_2O) and enzyme-catalyzed (formylglycine) reaction can also influence the $\beta_{leaving\ group}^{obs}$. Zalatan et al.[37] formulated these considerations to be able to calculate expected differences in leaving group dependence between enzyme-catalyzed ($\beta_{leaving\ group}^{Enz}$) and solution reactions ($\beta_{leaving\ group}^{solution}$) (eq 3). The expected change in leaving group dependence resulting from a change in nucleophile between the enzyme-catalyzed (fGly) and solution (H_2O) reaction is calculated from the difference in nucleophilicity ($pK_{nuc}^{Enz} - pK_{nuc}^{solution}$) weighed with the sensitivity of the leaving group dependence of the reaction type to a change in nucleophile (p_{xy}). The second of the contributing factors is leaving group-dependent binding of the ground state (GS, β_{bind}^{GS}) and TS (β_{bind}^{TS}). For k_{cat}/K_M-based $\beta_{leaving\ group}$ values the latter two are indistinguishable from each other and are treated as a single variable ($\sum\beta_{bind} = \beta_{bind}^{GS} + \beta_{bind}^{TS}$).

$$\beta_{leaving\ group}^{Enz} = \beta_{leaving\ group}^{solution} + p_{xy} \times (pK_{nuc}^{Enz} - pK_{nuc}^{solution}) + \beta_{bind}^{TS} + \beta_{bind}^{GS} \quad (3)$$

For *E. coli* AP, in particular, the interaction of the leaving group oxygen with one of the two Zn^{2+} ions during the GS and TS was thought to be mainly responsible for the $\sum\beta_{bind}$ of +0.33[89] (3 times larger than the expected contribution of the change in nucleophile from H_2O to the active site serine of +0.11). Selective removal of only the Zn^{2+} ion responsible for leaving group stabilization is not feasible, and therefore experimental assessment of these calculations was not possible. The assignment of the analogous positions of the nonbridging and bridging (leaving group) oxygens in an inorganic sulfate molecule with the active site residues of PAS (as shown in the X-ray structure,[44] Figure 1) was based on homology with structural data for the enzyme−substrate complex of an inactive variant of human arylsulfatase A.[75] The majority of the interactions with the nonbridging and leaving group oxygens are expected to be provided by amino acid side chains, which opens the possibility of assessing the importance of the correction factors of eq 3 experimentally by determining the leaving group dependence of active site mutants of PAS. To this end the nucleophile (fGly51) and a residue that directly interacts with it (H115) were mutated to assess the contribution of the nucleophile. Furthermore, several positively charged groups expected to provide charge compensation during the GS and TS by interacting with nonbridging (K113 and K375) and leaving group (H211 and K375) oxygens were removed by mutating the respective residues into alanine or leucine.

All mutants were purified to homogeneity and Michaelis−Menten parameters determined for the same series of sulfate monoesters (**1a**−**1l**, Scheme 1) as used with the wild-type enzyme. The mutations resulted in 1×10^3 to 1×10^8-fold drops in catalytic efficiencies (k_{cat}/K_M) for the various substrates (Tables S4−S8, Supporting Information). For mutants C51S and H211A k_{cat} was still independent of leaving group ability (Figure 2b,e, respectively), suggesting that, as in the wild-type enzyme, the leaving group-dependent step is not rate limiting. However, the k_{cat} for these mutants was reduced $\sim 1 \times 10^3$-fold (C51S) and $\sim 1 \times 10^5$-fold (H211A) compared to PAS WT. The K_M values for PAS C51S and H211A were within an order of magnitude of those for the wild-type enzyme (Tables S4 and S7) and, as observed for wild-type PAS, the $\beta_{leaving\ group}^{obs}$ values for k_{cat}/K_M and $1/K_M$ are nearly identical. For PAS K113L and H115A both k_{cat} and $1/K_M$ decreased with increasing leaving group ability (Figure 2c,d, Tables S5 and S6), albeit it only at the higher end of the pK_a spectrum for H115A. For PAS K375A k_{cat} decreases with increasing leaving group pK_a, indicating that the rate-limiting step is largely leaving group-dependent. The K_M values are increased $\sim 1 \times 10^3$-fold compared to the wild-type enzyme and are largely constant (varying in a range of 5−10 mM) for the substrates with a leaving group $pK_a > 8$ (Figure 2f, Table S8). The $\beta_{leaving\ group}^{obs}$ for k_{cat}/K_M is nearly identical to that for k_{cat} for $pK_a > 8$. As for PAS WT, the LFERs for k_{cat} and $1/K_M$ for PAS K113L, H115A, and K375A could be simulated based on assumed values for the pre-steady-state kinetic parameters (Figure S10, Supporting Information). In particular, for K113L and K375A the break in the LFER for k_{cat} could be explained by a change of the rate-limiting step with increasing $pK_a^{leaving\ group}$.

The $\beta_{leaving\ group}^{obs}$ of all active-site mutants was less negative than the $\beta_{leaving\ group}^{obs}$ for the wild type. $\Delta\beta_{leaving\ group}$ ($=\beta_{leaving\ group}^{obs\text{-}WT} - \beta_{leaving\ group}^{obs\ mutant}$) was calculated as the slope of the linear correlation of $\log[(k_{cat}/K_M)_{WT}/(k_{cat}/K_M)_{mutant}]$ versus $pK_a^{leaving\ group}$ (Table 2, Figure S11a). As described above the difference in leaving group dependencies between enzyme-catalyzed and uncatalyzed sulfate and phosphate monoester hydrolysis is influenced by the nature of the nucleophile and charge compensation effects (eq 3). On the basis of the pH-rate profile for PAS-catalyzed sulfate monoester hydrolysis the pK_{nuc} of the enzyme is expected to be less than 7.2.[1] The p_{xy} value for sulfate transfer is not known, but it is expected to be similar to the value for phosphate monoesters (0.013).[92] Assuming that the $pK_{nuc}^{Enz} \approx 6$ and $pK_{nuc}^{solution} = -1.7$ (nucleophile = H_2O), the effect of the change in nucleophile between the PAS WT-catalyzed and the solution reaction is expected to be $0.013 \times (6 - (-1.7)) = +0.10$. Assuming the difference in nucleophilicity between fGly (solution $pK_a \approx 13$−14[93]) and serine ($pK_a \approx 16$, similar to

DOI: 10.1021/acs.biochem.8b00996
Biochemistry 2019, 58, 1363−1378

Table 2. Effect of Mutations on Leaving Group Dependence for PAS-Catalyzed Sulfate Monoester Hydrolysis in PAS WT and K375A

mutation	reaction	effect in	$\Delta\beta_{leaving\ group}^{obs}$
C51S	**1a**–**1l**	WT	+0.10 ± 0.04[a]
	1a–**1d**	K375A	+0.01 ± 0.33[b]
K113L	**1c**–**1l**	WT	+0.24 ± 0.05[a]
H115A	**1a**, **1c**–**1l**	WT	+0.32 ± 0.03[a]
	1a–**1l**	K375A	+0.15 ± 0.05[b]
H211A	**1c**–**1l**	WT	+0.16 ± 0.07[a]
K375A	**1a**–**1e**	WT	+0.61 ± 0.03[a]

[a]Determined as the slope for $\log[(k_{cat}/K_M)_{WT}/(k_{cat}/K_M)_{mutant}]$ plotted versus leaving group pK_a (Figure S10a). [b]Determined as the slope for $\log[(k_{cat}/K_M)_{K375A}/(k_{cat}/K_M)_{double\ mutant}]$ plotted versus leaving group pK_a (Figure S10b, Supporting Information).

that of ethanol) in solution translates into the same difference in the enzyme active site, a small increase in the contribution of the nucleophile term in eq 3 is expected for mutant C51S. On the basis of this assumption the $\Delta\beta_{leaving\ group}^{WT\text{-}C51S}$ is expected to be small and negative. However, we measure a value of +0.10 (Table 2). Since fGly is interacting directly with the Ca^{2+} ion, changing it to a serine may cause a change in the charge compensation effects provided by the divalent cation, which could explain the positive value for $\Delta\beta_{leaving\ group}^{WT\text{-}C51S}$. Removal of H115 is expected to result in a slight increase in the pK_a of the nucleophile, again predicting a small negative $\Delta\beta_{leaving\ group}^{WT\text{-}H115A}$ as a result. However, the measured value of +0.32 suggests that any small effect of the mutation on the nucleophile term is overshadowed by a considerable decrease in $\sum\beta_{bind}$.

The removal of the residues that directly interact with the leaving group oxygen is expected to have a large effect on $\sum\beta_{bind}$, whereas groups that interact only with the nonbridging oxygens are expected to contribute to $\sum\beta_{bind}$ at ∼10% of the value expected for direct interactions with the leaving group oxygen.[37] Mutation of H211 resulted in a $\Delta\beta_{leaving\ group}^{WT\text{-}H211A}$ of only +0.16, even though this residue interacts exclusively with be the leaving group oxygen. Removal of the nearby K375 results in a $\Delta\beta_{leaving\ group}^{WT\text{-}K375A}$ of +0.61. Since the removal of a positive charge is expected to increase the pK_{nuc}^{Enz}, the actual effects on $\sum\beta_{bind}$ may be slightly higher than observed.

Taken together these data suggest that K375 is largely responsible for leaving group stabilization, either by electrostatic charge offset or by proton transfer. However, unlike in PTPase,[56] where a protonated aspartate performs the same function, its removal does not result in a near-complete abolition of the difference between $\beta_{leaving\ group}^{obs\text{-}Enz}$ and $\beta_{leaving\ group}^{obs\text{-}solution}$, since $\Delta\beta_{leaving\ group}^{PAS\ K375A\text{-}solution}$ = +0.87. Values of ca. +0.1–0.2 would be expected in case of complete removal of charge compensation on the leaving group as a result of the mutation (i.e., $\sum\beta_{bind}$ = 0, only the change in nucleophile results in a small positive $\Delta\beta_{leaving\ group}^{obs}$). This observation could be rationalized by partial compensation of the loss of charge offset (or of partial proton transfer) provided by K375 by nearby H211. The same phenomenon (i.e., that K375 partially assumes the role of H211) could explain the relatively small effect of mutation H211A on $\beta_{leaving\ group}^{obs}$. The combined effects of these two residues find support in the double mutant enzyme PAS H211A/K375A, for which no sulfatase activity was detectable (k_{cat}/K_M < 5 × 10^{-6} s^{-1} M^{-1} for sulfate monoester **1d**; see Supporting Information for consideration of the experimental detection limit). This observation strengthens the idea that the effect of each mutation is buffered by the nearby presence of a residue that can take over its function: if the measured reductions in activity for the single mutants were simply additive, the expected k_{cat}/K_M for sulfate monoester **1d** should be 2.6 × 10^{-3} s^{-1} M^{-1} (according to equation S21, Supporting Information) and still be detectable. By contrast, their cooperativity leads to a larger detrimental effect, when both are removed.

As discussed above the effect of leaving group-dependent ground- and transition-state binding ($\sum\beta_{bind}$) is expected to be modest for residues that interact mainly with the nonbridging oxygens: ∼10% (for all the nonbridging oxygens combined) of the value expected for leaving group oxygen.[89] This consideration suggests that the maximal combined effect of K113, K375, and Ca^{2+} on $\sum\beta_{bind}$ via interactions with the nonbridging oxygens is expected to be ca. +0.13 (10/110 × ($\beta_{leaving\ group}^{obs\text{-}WT}$ − $\beta_{leaving\ group}^{obs\text{-}solution}$) = 0.09 × (−0.33 − (−1.81)) = +0.13). Since removal of a positive charge is expected to increase the pK_{nuc} of the enzymatic reaction, the observed effect on $\sum\beta_{bind}$ of the interaction with nonbridging oxygens, as a result of removing any of these three functional groups, is expected to be less than +0.05. However, mutation K113L results in a $\Delta\beta_{leaving\ group}^{WT\text{-}K113L}$ of +0.24. This large effect partly explains why removal of H115 has an unexpectedly large $\Delta\beta_{leaving\ group}^{WT\text{-}H115A}$ of +0.32, since H115 and K113 interact closely in the three-dimensional structure of PAS. The large effect of mutations C51S, K113L, and H115A on PAS activity suggests that these mutations influence the interaction of the H211A/K375A pair with the leaving group oxygen. If the effects were electrostatic and isolated from the interactions with the leaving group oxygens, the effect of these mutations would be expected to be identical in K375A and WT; that is, these three mutations should be additive to mutation K375A. The combined effects of K113L and K375A result in completely inactive enzyme (k_{cat}/K_M < 5 × 10^{-6} s^{-1} M^{-1} for sulfate monoester **1d**), which is lower than the expected value (7.0 × 10^{-4} s^{-1} M^{-1}; based on eq S21, Supporting Information) for an additive effect of both mutations. This can be explained by interaction of both K113 and K375 with the nonbridging oxygens, in which case their simultaneous removal most likely results in complete abolition of substrate binding. The introduction of mutations C51S and H115A into the K375A variant does result in enzymes with detectable activities. However, the effect on the $\beta_{leaving\ group}^{obs}$ is much lower in the K375A mutant than in the wild-type enzyme, if present at all (C51S in K375A has no significant effect on $\beta_{leaving\ group}$; see Table 2 and Figure S10b for details). The nonadditive behavior suggests that the unexpectedly large value of $\Delta\beta_{leaving\ group}^{WT\ mutant}$ for both these mutations is due to their effect on the interactions between the leaving group oxygen and K375; that is, this effect cannot be achieved unless K375 is present. Possible explanations for this phenomenon are (i) changes in the overall electrostatic character of the active site as result of the mutations that decrease the strength of the interaction between K375 and the leaving group oxygen or (ii) changes in substrate positioning that cause the optimal configuration of the K375 leaving group oxygen paring to be distorted, resulting in a lower contribution of this interaction to TS stabilization.

In addition (or as an alternative) to the above considerations of charge compensation, changes in $\beta_{leaving\ group}^{obs}$ can also reflect

DOI: 10.1021/acs.biochem.8b00996
Biochemistry 2019, 58, 1363–1378

changes in the nature of the transition state. We discuss these aspects together with kinetic isotope effects below.

Kinetic Isotope Effects. Kinetic isotope effects were measured for the bridging (or leaving group) and nonbridging oxygens as well as the nitro group for enzyme-catalyzed hydrolysis of sulfate monoester **1d** and phosphate monoester **2d** (Figure 3; Chart S1, Supporting Information), to complement the Brønsted analysis above.[56,58] The KIE experiment requires turnover of approximately half of a 100 μmol sample of labeled substrate. With mutants of low activity this can require long reaction times, or unpractically large amounts of enzyme. For that reason, most but not all of the mutants for which kinetic data are presented have accompanying KIE data in Table 3.

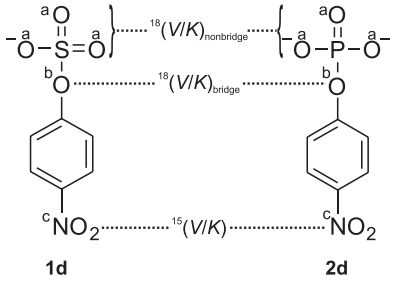

Figure 3. Positions for the KIE measurements in sulfate monoester **1d** and phosphate monoester **2d**. Effects were measured for the nonbridging oxygens (a, $^{18}O_{nonbridge}$ KIE), bridging oxygen (b, $^{18}O_{bridge}$ KIE), and for the nitro group (c, ^{15}N KIE). See Chart S1 (Supporting Information) for the structures of the labeled compounds used.

Table 3. Kinetic Isotope Effects for PAS-Catalyzed Hydrolysis of Sulfate Monoester 1d and Phosphate Monoester 2d

substrate	catalyst	$^{15}(V/K)$	$^{18}(V/K)_{bridge}$	$^{18}(V/K)_{nonbridge}$
1d	solution (neutral)[a]	1.0004 (1)	1.0101 (2)	1.0098 (3)
	solution (monoanion)[b]	1.0026 (1)	1.0210 (10)	0.9951 (3)
	WT	1.0006 (4)	1.0088 (9)	1.0064 (15)
	C51S	1.0012 (6)	1.0097 (19)	1.0039 (4)
	H115A	1.0013 (2)	1.0216 (17)	1.0004 (6)
	H211A[c]			
	K375A	1.0023 (5)	1.0244 (23)	0.9958 (11)
2d	solution (monoanion)[d]	1.0004 (2)	1.0087 (3)	1.0184 (5)
	solution (dianion)[d]	1.0028 (2)	1.0189 (5)	0.9994 (5)
	WT	1.0007 (4)	1.0102 (9)	0.9912 (8)

[a]Recorded in 10 N HCl, 15 °C.[78] [b]Recorded at pH 9.0, 85 °C.[78] [c]Activity too low to be determined. [d]Recorded at 95 °C.[53]

Because the KIEs were measured by the internal competition method, they describe effects on k_{cat}/K_M (or V/K),[94] encompassing steps from free enzyme and substrate up to the first irreversible step, regardless of which step in the full mechanism is rate-limiting. In the present case, as described above, this is representative of the rate constant for the first chemical step (k_2 in Figure 1c). Thus, the reported KIEs reflect the TS for the substrate reacting with the formyl glycine nucleophile, even though the overall rate-determining step is breakdown of the intermediate.

The expected ranges of the isotope effects in sulfate monoester **1d** and phosphate monoester **2d** and their interpretation have been discussed in detail previously.[80,95] The secondary KIE at the nitrogen atom, $^{15}(V/K)$, reports on negative charge development on the nitrophenolate leaving group in the transition state. The *p*-nitrophenolate anion has contributions from a quinonoid resonance form, with decreased N−O bond order and increased N−C bond order. Because N−O bonds have tighter vibrational frequencies, the nitrogen atom is more tightly bonded in neutral *p*-nitrophenol (or in substrates **1d** and **2d**) than in the phenolate anion.[96] Thus, the ^{15}N KIE for deprotonation of *p*-nitrophenol is normal. When protonation or other interactions maintain the leaving group in a neutral state, there is no isotope effect (KIE = unity). This KIE reaches its maximum value of ∼1.003, reflecting a full negative charge, when the leaving group in the TS has a very high degree of bond fission and no interactions neutralize the resulting charge. The KIE at the bridging oxygen atom, $^{18}(V/K)_{bridge}$, is a primary isotope effect that arises from S−O or P−O bond fission and is also affected by O−H bond formation, if the leaving group is simultaneously protonated in the TS. Bond fission produces normal isotope effects, primarily due to reduction of the stretching vibration in the TS as the force constant is lowered. Protonation of this atom in the TS gives rise to inverse effects, from the new vibrational modes introduced from the forming bond. A large body of data from phosphate and sulfate ester hydrolysis shows the isotope effect from P−O or S−O bond fission is normally larger in magnitude than the inverse effect from protonation. A normal $^{18}(V/K)_{bridge}$ effect near its maximum of 1.03 reflects a largely broken S−O or P−O bond in the TS, arising from loss of vibrations involving this bond. In native enzymes utilizing general acid catalysis, or uncatalyzed reactions under acidic conditions, the observed $^{18}(V/K)_{bridge}$ is reduced by protonation, as shown in Table 3.

The leaving group KIEs $^{15}(V/K)$ and $^{18}(V/K)_{bridge}$ report on how leaving group stabilization might be compromised by mutation. Loss of general or Lewis acid catalysis will result in increases in both of these KIEs relative to the native enzyme. The isotope effect on the nonbridging oxygen atoms, $^{18}(V/K)_{nonbridge}$, monitors the hybridization state of the transferring sulfuryl or phosphoryl group, which affects the P−O or S−O nonbridging bond orders and hence their vibrational frequencies. A loose transition state gives rise to slightly inverse effects as these bond orders increase. This isotope effect becomes increasingly normal (i.e., approaching or exceeding a value of 1) as the transition state grows more associative in nature.

The small $^{15}(V/K)$ of 1.0006 (Table 3), for PAS WT-catalyzed hydrolysis of sulfate monoester **1d** suggests nearly complete neutralization of the negative charge developing on the leaving group from S−O bond fission. Similar neutralization occurs by intramolecular pre-equilibrium proton transfer during the uncatalyzed hydrolysis of neutral sulfate monoesters under acidic conditions[78] ($^{15}(V/K)$ = 1.0004). The $^{18}(V/K)_{bridge}$ KIE for the PAS-catalyzed reaction is similar to that of the uncatalyzed hydrolysis of the neutral monoester[78] and the AP-catalyzed sulfate monoester hydrolysis[21] (Table 3, Figure 4a). In both cases significant masking of leaving group charge development occurs due to intramolecular proton transfer or interaction with a Lewis acid, respectively. The magnitude of $^{18}(V/K)_{bridge}$ is consistent with significant S−O_{bridge} bond fission concomitant with leaving group stabilization, either by interaction with a positively charged group (Lewis acid) or protonation. A similar observation has been made for phosphate

DOI: 10.1021/acs.biochem.8b00996
Biochemistry 2019, 58, 1363−1378

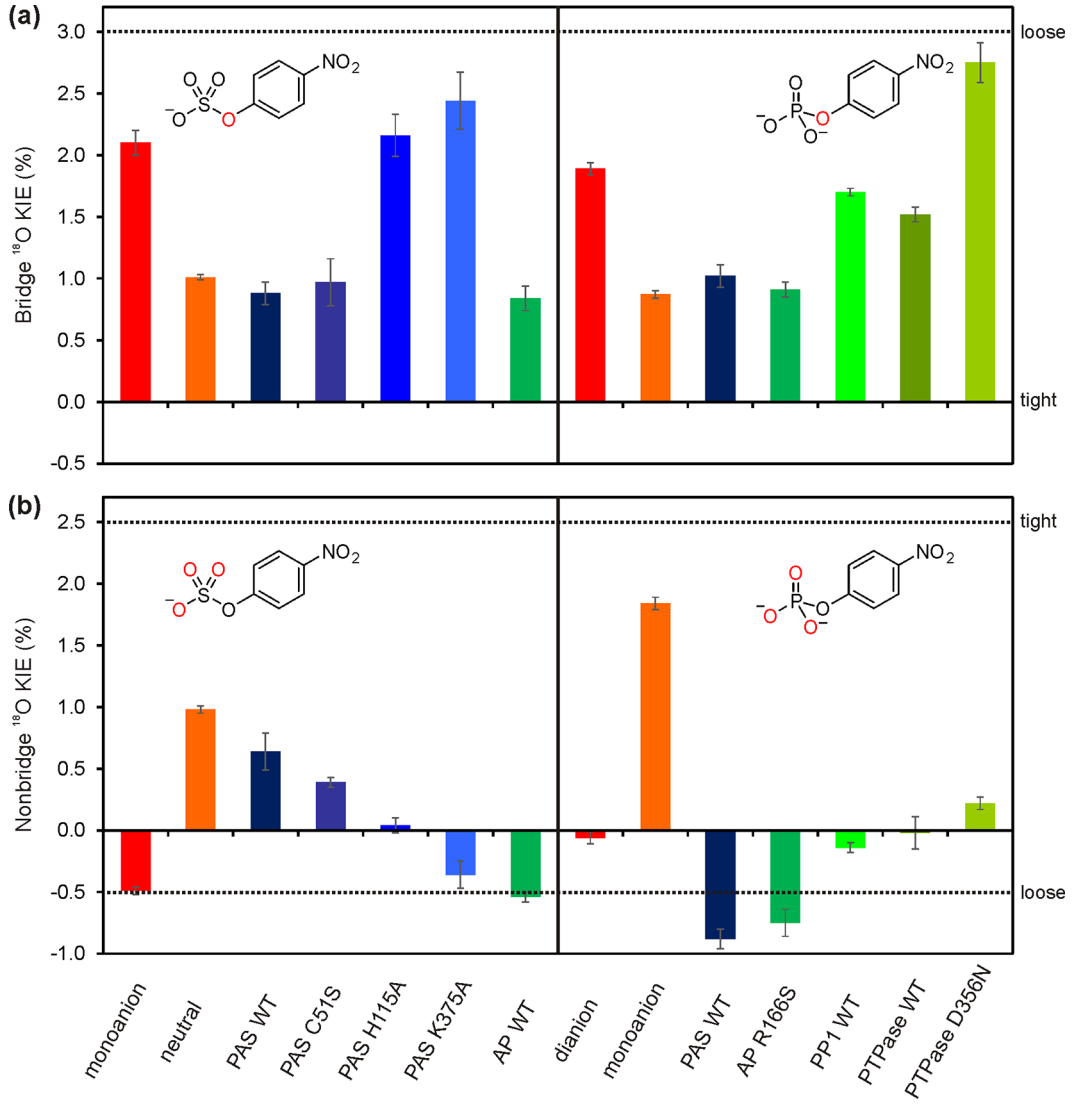

Figure 4. KIEs for PAS-catalyzed hydrolysis of sulfate monoester **1d** and phosphate monoester **2d**. The values are listed in Table 3 (PAS and solution data) and Table S15 (all other enzymatic data, Supporting Information). (**a**) The ^{18}O KIEs for the bridging (or leaving group) oxygen. (**b**) The ^{18}O KIEs for the nonbridging oxygens. The dotted lines indicate extremes of ^{18}O KIEs for tight (^{18}O bridge = 0%, ^{18}O nonbridge = +2.5%) and loose (^{18}O bridge = +3.0%, ^{18}O nonbridge = −0.5%) transition states.[80] AP: *E. coli* alkaline phosphatase,[21] PP1: Protein Phosphatase 1,[58] PTPase: *Yersinia* Protein Tyrosine Phosphatase.[54]

monoester hydrolysis catalyzed by AP,[21] protein phosphatase 1[58] (PP-1), and several protein-tyrosine phosphatases (PTPs)[51,52,54,55,97] (Figure 4a, Table S15).

In the PAS WT-catalyzed hydrolysis of phosphate monoester **2d**, the $^{15}(V/K)$ and $^{18}(V/K)_{bridge}$ KIEs also indicate near complete neutralization of the charge on the leaving group and significant P−O_{bridge} bond fission (Table 3, Figure 4a). The $^{18}(V/K)_{nonbridge}$ KIE for PAS WT-catalyzed hydrolysis of phosphate monoester **2d** was more inverse than for the uncatalyzed solution reaction of the dianion (0.9912 vs 0.9994; Table 3, Figure 4b) and is similar to the value for its hydrolysis by the superfamily member AP R166S (0.9925).[36] In the case of AP the inverse shift in this KIE was attributed to interactions of the phosphoryl group with the metal ions and hydrogen-bonding residues at the active site. In the PAS reaction similar interactions are possible (Figure 1). For the PAS WT-catalyzed hydrolysis of sulfate monoester **1d** the $^{18}(V/K)_{nonbridge}$ is normal (1.0064, or +0.64%, Table 3 and Figure 4b), in contrast to the inverse $^{18}(V/K)_{nonbridge}$ for the uncatalyzed hydrolysis of the **1d** monoanion[78] (−0.49%). This value is closer to the $^{18}(V/K)_{nonbridge}$ for the hydrolysis of the neutral sulfate monoester[78] (+0.98%). However, in this case, the normal KIE arises from deprotonation of the sulfuryl group (i.e., proton transfer from S−O−H to the leaving group). In previous investigations of the TS for enzymatic sulfate and phosphate transfer the drop in the normal $^{18}(V/K)_{bridge}$ was accompanied by a more inverse[21] or mostly unchanged $^{18}(V/K)_{nonbridge}$ KIE[51,52,54−56,58,97] (compared to the $^{18}(V/K)_{nonbridge}$ for uncatalyzed phosphate dianion hydrolysis; i.e., ≤0.9994), and suggests that the TS in these enzymatic reactions is still largely dissociative despite the less negative $\beta_{leaving\ group}^{obs}$ and drop in normal $^{18}(V/K)_{bridge}$ KIE compared to the uncatalyzed reaction, which arise from neutralization of the charge developing on the leaving group.

The normal $^{18}(V/K)_{nonbridge}$ is unlikely to arise from the same origin as in the uncatalyzed hydrolysis of the neutral sulfate monoester, since protonation of the sulfuryl group oxygens will not occur, except under extremely acidic conditions. A more

DOI: 10.1021/acs.biochem.8b00996
Biochemistry 2019, 58, 1363−1378

plausible explanation is that the PAS WT-catalyzed TS is more associative than the solution reaction of the monoanion. The latter scenario could also partly explain the unexpectedly large effect of the removal of residues that only interact indirectly with the nonbridging leaving group oxygen on $\beta_{leaving\ group}^{obs}$.

The PAS K375A mutation results in a reaction for which the $^{15}(V/K)$ and $^{18}(V/K)_{bridge}$ KIEs are largely identical to those of the uncatalyzed hydrolysis (Table 3, Figure 4b), suggesting this residue is largely responsible for leaving group neutralization in the TS. This is consistent with the effect of the mutation on the $\beta_{leaving\ group}^{obs}$ and similar to the value observed for the removal of an aspartic acid performing a similar role in PTPs.[52,54,55] The data suggest that this residue either protonates the leaving group directly or that its mutation results in a dislocation of H211 (Figure 1), interfering with its function in this role, implying synergy between these two residues, as discussed earlier. The $^{18}(V/K)_{nonbridge}$ for PAS K375A is identical to the uncatalyzed hydrolysis, which could be explained by the loss of coordination of K375 to the sulfuryl group.

The relatively modest effect of the C51S mutation on $^{15}(V/K)$ and $^{18}(V/K)_{bridge}$ compared to the wild-type reaction is consistent with the modest effect of this mutation on $\beta_{leaving\ group}^{obs}$. As stated above, the TS of the PAS WT-catalyzed sulfate monoester hydrolysis has a more associative character than in the uncatalyzed reaction; that is, the nature of the nucleophile is thought to be more important, based on the change to a normal $^{18}(V/K)_{nonbridge}$. However, the change in nucleophile from fGly to serine has a much smaller effect on $^{18}(V/K)_{nonbridge}$ than the removal of K375, which is thought to interact directly with the nonbridging oxygens (Figure 1).

The mutation of H115 to alanine has a large effect on the KIEs compared to WT, despite the absence of direct TS interaction between H115 and the substrate (Table 3, Figure 4). The $^{18}(V/K)_{bridge}$ is nearly as large as that observed for PAS K375A. The $^{15}(V/K)$ shows partial charge neutralization on the leaving group, intermediate between the WT reaction and that of K375A. A possible explanation is suboptimal orientation of the substrate relative to the residues mainly responsible for leaving group stabilization, K375 and H211. The reaction of the H115A mutant shows a $^{18}(V/K)_{nonbridge}$ that is also intermediate between the WT and K375A, also consistent with less than optimal coordination of the nonbridging oxygens to K375. The fact that mutation H115A has a larger effect on $^{18}(V/K)_{nonbridge}$ than C51S confirms that the large change in $^{18}(V/K)_{nonbridge}$ for the PAS WT-catalyzed reaction compared to the sulfate monoester monoanion uncatalyzed hydrolysis is most likely not dependent on the nucleophile but the result of interactions between the nonbridging oxygens and positively charged functional groups (K113, K375 and Ca^{2+}). The nature of the contribution of the latter interactions to TS stabilization appears to be unique for PAS WT-catalyzed sulfate monoester hydrolysis, since the effect of the enzyme on the $^{18}(V/K)_{nonbridge}$ for phosphate monoester hydrolysis is completely different. However, both reactions show a similar degree of leaving group stabilization.

Leaving Group Dependence in D_2O. The considerably less negative $\beta_{leaving\ group}^{obs}$ and a ^{15}N KIE near unity for the PAS WT-catalyzed sulfate monoester hydrolysis could be caused by protonation of the leaving group oxygen, as in PTPs.[52,54−56,59] Lewis acid charge neutralization by metal ions can have the same effect.[21] The available data for PAS all point to K375 as the main residue responsible for stabilization of charge that develops on the leaving group oxygen in the TS. Direct proton transfer involving lysine as the donor in enzyme active sites is rare, and charge compensation by Lewis acid interaction with the cationic charge of the proton shared between H211 and K375 is a potential alternative. The PAS WT-catalyzed sulfate monoester hydrolysis in D_2O is more sensitive to the leaving group ($\beta_{leaving\ group}$ is more negative) compared to the same reaction in H_2O (Figure S12). The observed difference in leaving group dependence ($\Delta\beta_{leaving\ group}^{H\text{-}D}$) is $+0.06 \pm 0.03$, which corresponds to a k_H/k_D ratio ranging from ~1.7 at $pK_a^{leaving\ group} = 5.5$ to ~3.3 at $pK_a^{leaving\ group} = 10$. These data suggest that, with increasing demand for leaving group stabilization, a proton transfer event becomes more rate-limiting. This would suggest that the degree of $S-O_{bridge}$ bond fission during the TS is reduced with increasing leaving group ability (i.e., $S-O_{bridge}$ bond fission is almost complete prior to proton transfer for the low pK_a leaving groups that require charge offset assistance less). However, the ^{15}N KIE for PAS WT-catalyzed hydrolysis of sulfate monoester **1d** ($pK_a = 7.02$) suggests almost complete charge compensation on the leaving group oxygen, suggesting K375 is mainly responsible for charge compensation without transferring its proton during catalysis. For PAS K375A, there is no difference in $\beta_{leaving\ group}^{obs}$ when recorded in H_2O or D_2O (Figure S13). However, a pK_a-independent k_H/k_D of ~2 for all reactions was observed, suggesting that a leaving group independent proton transfer event is rate-limiting for this mutant. The solvent isotope effect is consistent with the suggested catalytic role for K375 as the main residue responsible for leaving group stabilization during bond breaking in the TS, since any leaving group-dependent proton transfer event will most likely be fast compared to the severely slowed $S-O_{bridge}$ bond fission. Indeed, the heavy-atom isotope effects suggest that these two events occur in the same step.

IMPLICATIONS AND CONCLUSIONS

Assignment of Catalytic Roles to Active-Site Residues. A mechanistic pathway for PAS WT-catalyzed sulfate monoester hydrolysis (Figure 1b) had been suggested by structural analysis but can now be firmly established on the basis of the results presented in this study, including a reassessment of the contributions of the active-site residues. The presence of nine highly interconnected polar residues and a divalent metal cation, all of which could contribute to catalysis, makes assignment to specific function necessarily difficult, even when a high-resolution structure is available and patterns of amino acid conservation can be discerned.[98] The importance of each of these residues was further established in mutational scanning experiments with hASA (by changing them to either asparagine or aspartate),[49] but the observed v_{max} decreases and K_M increases implied that each of them was critical, leaving an ambiguity about their respective roles. An abundance of potentially functional residues is frequently observed. Indeed, such abundance has been convincingly explained by Kraut et al.[99] to be a result of the cooperativity of active sites that prevents a simple quantitative assignment of mechanistic contributions to individual residues. This present work exemplifies how LFERs can be employed to probe the role of catalytic residues comparatively in mutants, providing insights that amino acid scanning experiments evaluated by measurement of Michaelis−Menten parameters for one substrate do not provide. For example, leaving group stabilization by the proposed general acid H211 is much less important than that of K375 (based on the much smaller effect on $\beta_{leaving\ group}^{obs}$ upon alanine scanning).

DOI: 10.1021/acs.biochem.8b00996
Biochemistry 2019, 58, 1363−1378

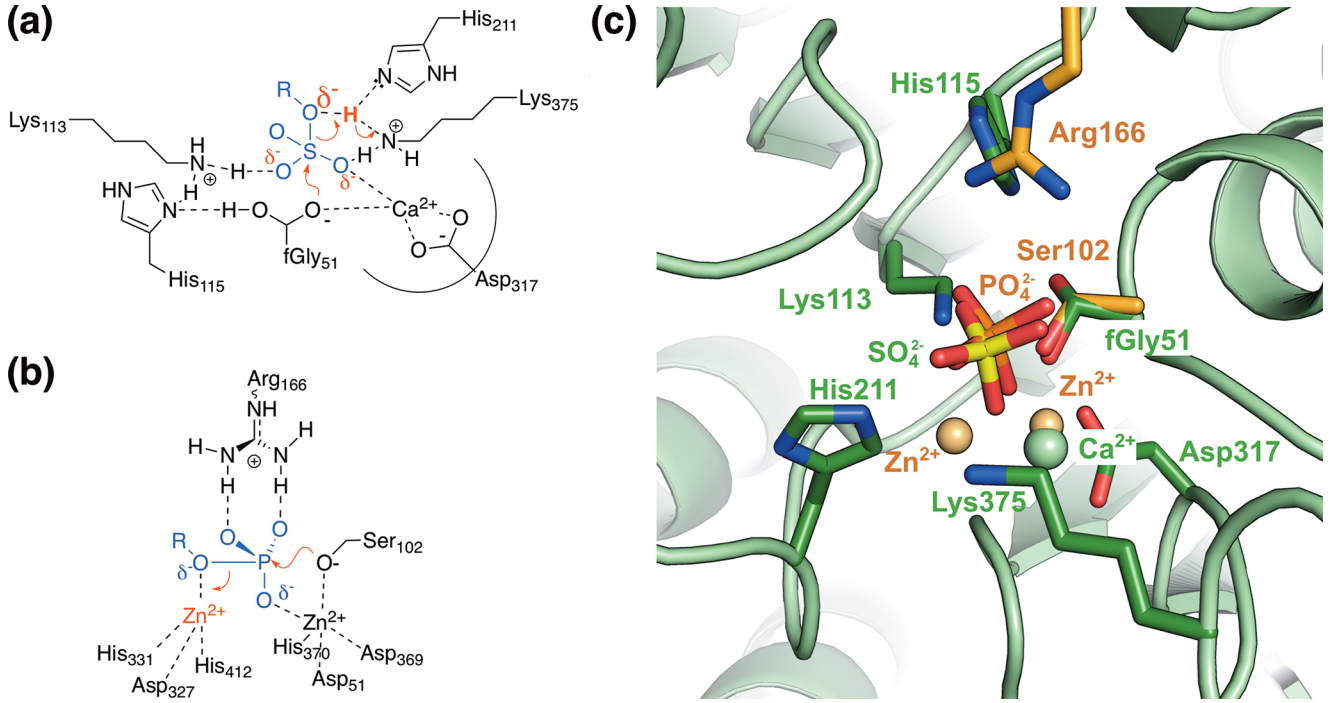

Figure 5. Comparison of mechanisms of leaving group stabilization in the transition states of sulfate monoester hydrolysis by PAS and phosphate monoester hydrolysis by alkaline phosphatase. (**a**) During fission of the sulfate ester bond negative charge develops on the leaving group and is offset by a proton, held by the H211−K375 pair. (**b**) In *Ec*AP[26,29] the charge developing on the leaving group as a serine nucleophile attacks is offset by a metal ion. (**c**) Structural superposition of PAS[44] (pdb entry 1HDH) and AP[100] (3TG0), including bound product in the active site (inorganic sulfate and phosphate, respectively. The functionally homologous residues align well, showing that the second divalent metal ion (Zn^{2+}) of AP is providing charge offset in a similar position as the proton held by H211 and K375 in PAS.

The LFERs serve to measure the effective charge "seen" at the leaving group oxygen on moving from ground to transition state[105] and quantify the charge compensation achieved by the enzyme via its side chains: in the absence of a charge-compensating residue a larger charge is seen at this oxygen. The combined effect of removing both these residues was larger than the sum of its effects in wild-type enzyme, suggesting a high degree of interdependence between them with regard to leaving group stabilization, possibly by sharing a proton (Figure 5). The LFERs for k_{cat} and $1/K_M$ for PAS WT-catalyzed sulfate monoester hydrolysis and the pre-steady-state measurements with sulfate monoester **1d** suggest that the leaving group-dependent sulfate ester bond fission (S−O_{bridge} fission; step 1 in Figure 1b) is much faster than the cleavage of the hemiacetal intermediate (step 2, Figure 1b).

The strongest effect on leaving group-dependent catalysis was seen for the K375A mutants ($\Delta\beta_{leaving\ group}^{obs}$ = +0.61, Figure 2f, Table 2), further underlining that K375 is the most important residue for stabilization of the negative charge that develops on the leaving group oxygen during catalysis. This conclusion was also supported by the following observations: (i) The ^{15}N and $^{18}O_{bridge}$ KIEs for mutant K375A are essentially the same as for the solution reaction. The wild type showed almost complete charge compensation on the leaving group (^{15}N KIE essentially unity) and a lowered normal $^{18}O_{brigde}$ KIE (Table 3, Figure 4). (ii) For PAS K375A the leaving group-dependent step becomes increasingly more rate-limiting with decreasing leaving group ability (Figures 2f and S10b), pointing to its involvement in leaving group stabilization. (iii) The unexpectedly large effects on $\beta_{leaving\ group}^{obs}$ for active site mutants C51S and H115A are dependent on the presence of K375 (Table 2), suggesting that the main function of the other active-site residues is to position the substrate for optimal interaction with K375. (iv) Structural alignment of PAS[44] with AP[100] shows that K375 occupies a similar position as the divalent metal ion thought to provide leaving group stabilization in AP (Figure 5).

Compensation of charge development on the leaving group oxygen by an amino acid side chain may be expected to involve direct protonation of the leaving group oxygen. The cleavage of this S−O_{bridge} ester is dependent on, and occurs in concert with, a near-complete neutralization of the charge on the leaving group for sulfate monoester **1d** ($pK_a^{leaving\ group}$ = 7.03), as evidenced by a ^{15}N KIE near unity (Table 3). This would suggest near-complete proton transfer during the TS, but transfer of the proton would only occur once the S−O_{bridge} bond cleavage is well advanced, if at all (Figure 5a,b). Charge compensation at the leaving group oxygen is nearly complete for PAS WT-catalyzed hydrolysis of sulfate monoester **1d**. As the proton is shared between H211 and K375 (Figure 5a,b) it may be that actual proton donation from lysine does not take place, and instead transfer to H211 results in the observed compensation. Comparison of the leaving group dependences in H_2O and D_2O showed an increasing k_H/k_D ratio for k_{cat}/K_M with decreasing leaving group ability (Figure S12, Supporting Information), suggesting that proton transfer is becoming increasingly more important for S−O_{bridge} ester bond fission. The absence of the leaving group-dependent change in k_H/k_D for PAS K375A (Figure S13) further supports the importance of K375 for S−O_{bridge} bond fission, since it is in agreement with S−O_{bridge} ester bond fission being fully rate-limiting for leaving group departure in this mutant. (This solvent isotope effect is relevant for the first chemical step, while the isotope effect on k_{cat} reflects the overall rate-determining step, i.e., breakdown of the intermediate).

DOI: 10.1021/acs.biochem.8b00996
Biochemistry 2019, 58, 1363−1378

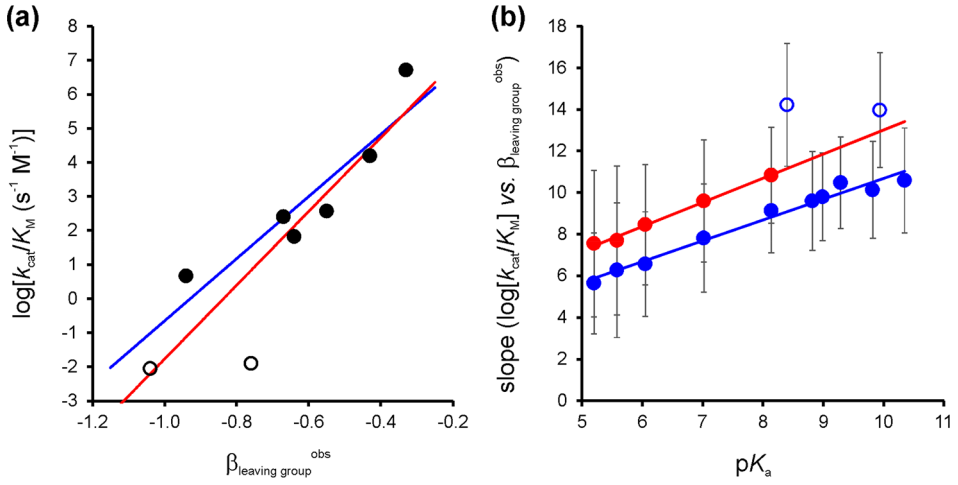

Figure 6. PAS variants with lower catalytic efficiencies are more sensitive to the leaving group ability. (**a**) Correlation between catalytic efficiency (represented by log[k_{cat}/K_M]) and leaving group dependency ($\beta_{leaving\ group}^{obs}$) of the various PAS variants (closed symbols: PAS WT and its single mutants, open symbols: double mutants) for 3-nitrophenyl sulfate **1e**. Linear correlations including *all* variants (red line, $R^2 = 0.79$; $p = 0.0033$) and only based on the single mutants and wild type (i.e., excluding the open symbols; blue line, $R^2 = 0.83$; $p = 0.011$) show slopes of 10.8 ± 2.3 and 9.1 ± 2.0, respectively. (**b**) Correlation between the response slope as shown in (**a**) and pK_a values of the substrate's leaving group (see Figure S14 for the corresponding red and blue correlation lines from which the slopes were obtained). The slopes for sulfate monoesters **1f** and **1k** (open blue symbols) clearly deviate from the observed trend (suggesting idiosyncratic active-site interactions) and were therefore not included in the fit (see Figure S15, Supporting Information, for a fit that includes all data points). Red fit: slope: 1.16 ± 0.05; R^2: 0.99; p: 2.2×10^{-4}. Blue fit: slope: 1.0 ± 0.06; R^2: 0.97; p: $<1 \times 10^{-4}$.

An alternative mechanistic scenario in which additional steps prior to the first irreversible S−O_{bridge} ester bond fission are rate-limiting for wild type, but the chemical step becomes limiting in a mutant, may be considered. Such an explanation has been advanced for FLAP endonuclease, where pH-rate profiles suggested rate-limiting physical steps after substrate binding resulted in a commitment to catalysis that suppressed the magnitude of $\beta_{leaving\ group}^{obs}$ and was reduced or eliminated by a mutation that slowed the chemistry step.[101] However, this scenario is inconsistent with the observed KIEs on PAS catalysis. A commitment factor would reduce all the observed KIEs in equal proportion.[94,102] Thus, if making the chemical step more rate-limiting (reducing a commitment factor) was the cause of the larger Brønsted slope, the KIEs would increase in the same proportion. Instead, the K375A mutant reaction gives a ^{15}N KIE that is fourfold higher than wild-type PAS; the bridge ^{18}O effect is 2.8-fold greater; and the nonbridge ^{18}O effect goes from normal to inverse. The substrates in FLAP and PAS also show significant differences: DNA substrates of FLAP may require unpairing or helical arch ordering, whereas for the small-molecule substrates of PAS no analogous steps are conceivable. In addition, the high K_M values are consistent with reversibility and a rapid equilibrium between bound and unbound states (contrasting with the nanomolar binding in FLAP). The LFERs and KIEs for PAS use k_{cat}/K_M comparisons that reflect the first irreversible step of the reaction, which thus is unlikely to be associated with binding.

Although the exact residues and functional groups involved differ between several previously characterized phosphatases[21,23,24,33,36,51,52,54−56,58,59,97] and PAS, all these enzymes rely on leaving group stabilization by charge compensation, resulting in less negative $\beta_{leaving\ group}^{obs}$ values and lowered, but still normal, $^{18}O_{bridge}$ KIEs. However, the KIEs for PAS are consistent with a more associative mechanism than previously reported phosphatases, because of the observed change of $^{18}O_{nonbrigde}$ KIE from inverse (−0.49%) to normal (+0.62%) compared to the solution reaction (Table 3, Figure 4b). In phosphatases the small inverse $^{18}O_{nonbridge}$ KIE was either more inverse[21] or virtually unchanged[51,52,54,55,58,97] (Figure 4b, Table S15). The possible change from a dissociative to a more associative TS does not apply to all PAS-catalyzed conversions, since the promiscuous enzyme-catalyzed hydrolysis of phosphate monoester **2d** showed a more inverse $^{18}O_{nonbridge}$. Enzymatic specificity toward sulfate over phosphate monoester cannot be primarily based on overall charge, demand for leaving group stabilization, or nucleophile strength, since these either provide no discrimination or will favor the more highly charged phosphate monoesters. The difference in effect on the $^{18}O_{nonbridge}$ KIE suggests that the subtle differences in geometry between the S−$O_{nonbridge}$ and P−$O_{nonbridge}$ bonds are responsible for making PAS specific toward sulfate monoesters.

Relationship to Computational Studies. The existence of computational studies attempting to model aspects of PAS catalysis *in silico*[38,42,43] provides an opportunity for a comparison of their conclusions with our experimental results. One report has taken a shortening of the S−O_{lg} bond distances (i.e., the $^{18}O_{bridge}$ in our study) as an indication for a shift to a more associative transition state.[38] However, these distances are not equivalent to shifts in TS. We find that the $^{18}O_{bridge}$ KIE is similar in both sulfate monoesters and phosphate monoesters, yet the nonbridging oxygen data (for which no computational results are available) differ widely. Importantly, only limited information on the individual contributions of active-site residues has been provided by computational studies. The residue that we show is central to both leaving group stabilization and shifting the nature of the TS for PAS-catalyzed sulfate monoester hydrolysis, K375, has not been discussed in the context of quantum mechanics/molecular mechanics (QM/MM) studies. Instead, Marino et al.[42] highlight the effect of H211 but assign its role as the sole general acid catalyst, while no such effect is ascribed to K375. Here, and in the work of Luo et al.,[38] residues that—in our analysis—are assigned only indirect roles affecting the nature of the TS and leaving group stabilization (K113,

DOI: 10.1021/acs.biochem.8b00996
Biochemistry 2019, 58, 1363−1378

H115, fGly51) feature more prominently. A third study[43] uses molecular dynamics simulations (based on active-site group ground-state pK_a values validated by PROPKA) to define a model that features K375 but not His211.

In computational studies with AP different authors obtained diverging predictions for enzymatic TSs that were either more associative[40] or more dissociative.[27] It is possible that the calculated relatively flat calculated energy surfaces (e.g., as shown in refs 39 and 103) make precise assignment of a TS position in More O'Ferrall/Jencks-type diagrams difficult *in silico*, as many energetically near-equivalent paths of bond-making and breaking seem to exist, yet these ambiguities may also be artifacts of the computational methods. Experimentally the notion of flat calculated energy surfaces is not supported: even in promiscuous enzymes the nature of the TS is close to that in solution,[23,32,36,37] suggesting it is hard to change. Computational results from modeling physical processes are not direct experimental observations and should not be used as substitutes of experimental reality. A more confident assignment of the nature of the TS requires resolution by experimental evidence of the sort presented here, that is, a kinetic analysis involving juxtapositions of LFERs and KIEs.

In comparing experimental and computational results it is important to bear in mind that in *in silico* work ground-state binding effects (contributing to K_M) are excluded and that elementary rate constants are calculated that may be implicit in Michaelis−Menten parameters but hard to disentangle. Multiple potentially rate-limiting steps may make these parameters complex functions of rate constants, preventing straightforward reconciliation of data. In some cases the computed energy levels do not reproduce the actually measured rates, indicating possible shortcomings in capturing the solution reaction,[103] but in the case of enzymatic reactions—also leading to postulation of different rate limiting steps. For example, the rate-limiting step of the PAS reaction had been predicted to be k_2,[42] which our analysis suggests to be incorrect. Our stopped-flow data suggest that k_2 (i.e., the relevant step in the LFERs) is at least 100-fold faster than k_{cat}. All these factors necessitate the judicious evaluation of both experimental and computational data with respect to functional conclusions, with many aspects necessitating experimental confirmation or resolution.

A Quantitative Measure for the Efficiency of General Acid or Charge Compensation Catalysis. The correlation of reaction rates and the measured values for $\beta_{\text{leaving group}}^{\text{obs}}$ (Figure 6) establishes a direct link between catalytic effects by charge compensation (and/or proton transfer) and catalytic efficiency: the more the catalytic effect of the protonation of an active site group is removed (as indicated by larger effective charge changes at the leaving group oxygen), the more the overall rate suffers. This effect is more pronounced for unreactive substrates that require interaction with the proton held by K375 and H211 to a greater extent (Figure S15), such as the presumed natural substrates, sulfated sugars.

The correlation of catalyst and substrate reactivity provides a further measure of sensitivity of catalysis to substrate reactivity changes and should be used to quantitatively assess the efficiency of general acid catalysis. In the future it will be interesting to contrast slopes in such double reactivity plots (as in Figure 6b) for several enzyme systems and use its slopes to quantify the sensitivity of catalytic effects in different active site arrangements.

More generally, this work shows that physical-organic approaches can continue to contribute to the understanding of enzyme catalysis[104] by providing a quantitative picture of elusive transition-state interactions, through the measurement of effective charge changes via Brønsted plots.[105] These, combined with isotope effects studies, are applied here systematically for the first time to studies of mutational effects to quantitatively assess the individual involvement of particular residues in PAS catalysis.

■ ASSOCIATED CONTENT

Supporting Information

The Supporting Information is available free of charge on the ACS Publications website at DOI: 10.1021/acs.biochem.8b00996.

Synthetic procedures, mathematical descriptions for enzyme kinetics and expected detection limits, determination of kinetic isotope effects, and data analysis. Michaelis−Menten plots for sulfate substrates hydrolyzed by PAS WT, tables of experimentally measured steady-state kinetic parameters, additional LFERs, stopped flow data, and primers used for mutant construction (PDF)

■ AUTHOR INFORMATION

Corresponding Authors

*E-mail: fh111@cam.ac.uk. (F.H.)
*E-mail: alvan.hengge@usu.edu. (A.C.H.)

ORCID

Bert van Loo: 0000-0003-4253-2163
Alvan C. Hengge: 0000-0002-5696-2087
Florian Hollfelder: 0000-0002-1367-6312

Present Addresses

§Institute for Evolution and Biodiversity, University of Münster, Germany.
‖Faculty of Tropical Medicine, Mahidol University, Thailand.
⊥Institute of Biochemistry, Faculty of Medicine, University of Ljubljana, Slovenia.

Funding

This research was funded by the Biological and Biotechnological Research Council (BBSRC, BB/I004327/1) and the Engineering and Physical Sciences Research Council (EPSRC, EP/E019390/1) and NIH grant GM 47292 to A.C.H.; F.H. is an ERC Investigator (695669); U.B. received a studentship from the Royal Thai Government; and M.G. was supported by a postdoctoral Marie-Curie fellowship from the EU.

Notes

The authors declare no competing financial interest.

■ ACKNOWLEDGMENTS

We thank M. Hyvonen for his help in the preparation of structural figures.

■ ABBREVIATIONS

AP, alkaline phosphatase; LFER, linear free energy relationship; KIE, kinetic isotope effect; PAS, *Pseudomonas aeruginosa* arylsulfatase.

■ REFERENCES

(1) Olguin, L. F., Askew, S. E., O'Donoghue, A. C., and Hollfelder, F. (2008) Efficient catalytic promiscuity in an enzyme superfamily: an arylsulfatase shows a rate acceleration of 10^{13} for phosphate monoester hydrolysis. *J. Am. Chem. Soc. 130*, 16547−16555.

DOI: 10.1021/acs.biochem.8b00996
Biochemistry 2019, 58, 1363−1378

(2) van Loo, B., Bayer, C. D., Fischer, G., Jonas, S., Valkov, E., Mohamed, M. F., Vorobieva, A., Dutruel, C., Hyvonen, M., and Hollfelder, F. (2019) Balancing specificity and promiscuity in enzyme evolution: multidimensional activity transitions in the alkaline phosphatase superfamily. *J. Am. Chem. Soc. 141*, 370−387.
(3) Edwards, D. R., Lohman, D. C., and Wolfenden, R. (2012) Catalytic proficiency: the extreme case of S-O cleaving sulfatases. *J. Am. Chem. Soc. 134*, 525−531.
(4) van Loo, B., Schober, M., Valkov, E., Heberlein, M., Bornberg-Bauer, E., Faber, K., Hyvonen, M., and Hollfelder, F. (2018) Structural and Mechanistic Analysis of the Choline Sulfatase from *Sinorhizobium melliloti*: A Class I Sulfatase Specific for an Alkyl Sulfate Ester. *J. Mol. Biol. 430*, 1004−1023.
(5) Haag, E. S., and Raff, R. A. (1998) Isolation and characterization of three mRNAs enriched in embryos of the direct-developing sea urchin *Heliocidaris erythrogramma*: evolution of larval ectoderm. *Dev. Genes Evol. 208*, 188−204.
(6) Sasaki, H., Yamada, K., Akasaka, K., Kawasaki, H., Suzuki, K., Saito, A., Sato, M., and Shimada, H. (1988) cDNA cloning, nucleotide sequence and expression of the gene for arylsulfatase in the sea urchin (*Hemicentrotus pulcherrimus*) embryo. *Eur. J. Biochem. 177*, 9−13.
(7) Yamada, K., Akasaka, K., and Shimada, H. (1989) Structure of sea-urchin arylsulfatase gene. *Eur. J. Biochem. 186*, 405−410.
(8) Yang, Q., Angerer, L. M., and Angerer, R. C. (1989) Structure and tissue-specific developmental expression of a sea urchin arylsulfatase gene. *Dev. Biol. 135*, 53−65.
(9) Lai, J., Chien, J., Staub, J., Avula, R., Greene, E. L., Matthews, T. A., Smith, D. I., Kaufmann, S. H., Roberts, L. R., and Shridhar, V. (2003) Loss of HSulf-1 up-regulates heparin-binding growth factor signaling in cancer. *J. Biol. Chem. 278*, 23107−23117.
(10) Morimoto-Tomita, M., Uchimura, K., Werb, Z., Hemmerich, S., and Rosen, S. D. (2002) Cloning and characterization of two extracellular heparin-degrading endosulfatases in mice and humans. *J. Biol. Chem. 277*, 49175−49185.
(11) Obaya, A. J. (2006) Molecular cloning and initial characterization of three novel human sulfatases. *Gene 372*, 110−117.
(12) Scott, W. A., and Metzenberg, R. L. (1970) Location of Aryl Sulfatase in Conidia and Young Mycelia of *Neurospora crassa*. *J. Bacteriol. 104*, 1254−1265.
(13) Ratzka, A., Vogel, H., Kliebenstein, D. J., Mitchell-Olds, T., and Kroymann, J. (2002) Disarming the mustard oil bomb. *Proc. Natl. Acad. Sci. U. S. A. 99*, 11223−11228.
(14) Wittstock, U., Fischer, M., Svendsen, I., and Halkier, B. A. (2000) Cloning and characterization of two cDNAs encoding sulfatases in the Roman snail, *Helix pomatia*. *IUBMB Life 49*, 71−76.
(15) Govan, J. R., and Deretic, V. (1996) Microbial pathogenesis in cystic fibrosis: mucoid *Pseudomonas aeruginosa* and *Burkholderia cepacia*. *Microbiol. Rev. 60*, 539−574.
(16) Jansen, H. J., Hart, C. A., Rhodes, J. M., Saunders, J. R., and Smalley, J. W. (1999) A novel mucin-sulphatase activity found in *Burkholderia cepacia* and *Pseudomonas aeruginosa*. *J. Med. Microbiol. 48*, 551−557.
(17) Piotrowski, J., Slomiany, A., Murty, V. L., Fekete, Z., and Slomiany, B. L. (1991) Inhibition of *Helicobacter pylori* colonization by sulfated gastric mucin. *Biochem. Int. 24*, 749−756.
(18) Diez-Roux, G., and Ballabio, A. (2005) Sulfatases and human disease. *Annu. Rev. Genomics Hum. Genet. 6*, 355−379.
(19) Ghosh, D. (2007) Human sulfatases: a structural perspective to catalysis. *Cell. Mol. Life Sci. 64*, 2013−2022.
(20) von Figura, K., Schmidt, B., Selmer, T., and Dierks, T. (1998) A novel protein modification generating an aldehyde group in sulfatases: its role in catalysis and disease. *BioEssays 20*, 505−510.
(21) Catrina, I., O'Brien, P. J., Purcell, J., Nikolic-Hughes, I., Zalatan, J. G., Hengge, A. C., and Herschlag, D. (2007) Probing the origin of the compromised catalysis of *E. coli* alkaline phosphatase in its promiscuous sulfatase reaction. *J. Am. Chem. Soc. 129*, 5760−5765.
(22) Hall, A. D., and Williams, A. (1986) Leaving group dependence in the phosphorylation of *Escherichia coli* alkaline phosphatase by monophosphate esters. *Biochemistry 25*, 4784−4790.
(23) Hollfelder, F., and Herschlag, D. (1995) The nature of the transition state for enzyme-catalyzed phosphoryl transfer. Hydrolysis of *O*-aryl phosphorothioates by alkaline phosphatase. *Biochemistry 34*, 12255−12264.
(24) Holtz, K. M., Catrina, I. E., Hengge, A. C., and Kantrowitz, E. R. (2000) Mutation of Arg-166 of alkaline phosphatase alters the thio effect but not the transition state for phosphoryl transfer. Implications for the interpretation of thio effects in reactions of phosphatases. *Biochemistry 39*, 9451−9458.
(25) Holtz, K. M., and Kantrowitz, E. R. (1999) The mechanism of the alkaline phosphatase reaction: insights from NMR, crystallography and site-specific mutagenesis. *FEBS Lett. 462*, 7−11.
(26) Holtz, K. M., Stec, B., and Kantrowitz, E. R. (1999) A model of the transition state in the alkaline phosphatase reaction. *J. Biol. Chem. 274*, 8351−8354.
(27) Hou, G., and Cui, Q. (2012) QM/MM analysis suggests that Alkaline Phosphatase (AP) and nucleotide pyrophosphatase/phosphodiesterase slightly tighten the transition state for phosphate diester hydrolysis relative to solution: implication for catalytic promiscuity in the AP superfamily. *J. Am. Chem. Soc. 134*, 229−246.
(28) Hou, G., and Cui, Q. (2013) Stabilization of different types of transition states in a single enzyme active site: QM/MM analysis of enzymes in the alkaline phosphatase superfamily. *J. Am. Chem. Soc. 135*, 10457−10469.
(29) Kim, E. E., and Wyckoff, H. W. (1991) Reaction mechanism of alkaline phosphatase based on crystal structures. Two-metal ion catalysis. *J. Mol. Biol. 218*, 449−464.
(30) Nikolic-Hughes, I., O'Brien, P. J., and Herschlag, D. (2005) Alkaline phosphatase catalysis is ultrasensitive to charge sequestered between the active site zinc ions. *J. Am. Chem. Soc. 127*, 9314−9315.
(31) Nikolic-Hughes, I., Rees, D. C., and Herschlag, D. (2004) Do electrostatic interactions with positively charged active site groups tighten the transition state for enzymatic phosphoryl transfer? *J. Am. Chem. Soc. 126*, 11814−11819.
(32) O'Brien, P. J., and Herschlag, D. (1999) Does the Active Site Arginine Change the Nature of the Transition State for Alkaline Phosphatase-Catalyzed Phosphoryl Transfer? *J. Am. Chem. Soc. 121*, 11022−11023.
(33) O'Brien, P. J., and Herschlag, D. (2002) Alkaline phosphatase revisited: hydrolysis of alkyl phosphates. *Biochemistry 41*, 3207−3725.
(34) O'Brien, P. J., Lassila, J. K., Fenn, T. D., Zalatan, J. G., and Herschlag, D. (2008) Arginine coordination in enzymatic phosphoryl transfer: evaluation of the effect of Arg166 mutations in *Escherichia coli* alkaline phosphatase. *Biochemistry 47*, 7663−7672.
(35) Simopoulos, T. T., and Jencks, W. P. (1994) Alkaline phosphatase is an almost perfect enzyme. *Biochemistry 33*, 10375−10380.
(36) Zalatan, J. G., Catrina, I., Mitchell, R., Grzyska, P. K., O'Brien, P. J., Herschlag, D., and Hengge, A. C. (2007) Kinetic isotope effects for alkaline phosphatase reactions: implications for the role of active-site metal ions in catalysis. *J. Am. Chem. Soc. 129*, 9789−9798.
(37) Zalatan, J. G., and Herschlag, D. (2006) Alkaline phosphatase mono- and diesterase reactions: comparative transition state analysis. *J. Am. Chem. Soc. 128*, 1293−1303.
(38) Luo, J., van Loo, B., and Kamerlin, S. C. (2012) Catalytic promiscuity in *Pseudomonas aeruginosa* arylsulfatase as an example of chemistry-driven protein evolution. *FEBS Lett. 586*, 1622−1630.
(39) Luo, J., van Loo, B., and Kamerlin, S. C. (2012) Examining the promiscuous phosphatase activity of *Pseudomonas aeruginosa* arylsulfatase: a comparison to analogous phosphatases. *Proteins: Struct., Funct., Genet. 80*, 1211−1226.
(40) Lopez-Canut, V., Roca, M., Bertran, J., Moliner, V., and Tunon, I. (2011) Promiscuity in alkaline phosphatase superfamily. Unraveling evolution through molecular simulations. *J. Am. Chem. Soc. 133*, 12050−12062.
(41) Barrozo, A., Duarte, F., Bauer, P., Carvalho, A. T., and Kamerlin, S. C. (2015) Cooperative Electrostatic Interactions Drive Functional Evolution in the Alkaline Phosphatase Superfamily. *J. Am. Chem. Soc. 137*, 9061−9076.

DOI: 10.1021/acs.biochem.8b00996
Biochemistry 2019, 58, 1363−1378

(42) Marino, T., Russo, N., and Toscano, M. (2013) Catalytic mechanism of the arylsulfatase promiscuous enzyme from *Pseudomonas aeruginosa*. *Chem. - Eur. J. 19*, 2185−2192.
(43) Uduwela, D. R., Pabis, A., Stevenson, B. J., Kamerlin, S. C. L., and McLeod, M. D. (2018) Enhancing the Steroid Sulfatase Activity of the Arylsulfatase from *Pseudomonas aeruginosa*. *ACS Catal. 8*, 8902−8914.
(44) Boltes, I., Czapinska, H., Kahnert, A., von Bulow, R., Dierks, T., Schmidt, B., von Figura, K., Kertesz, M. A., and Uson, I. (2001) 1.3 Å structure of arylsulfatase from *Pseudomonas aeruginosa* establishes the catalytic mechanism of sulfate ester cleavage in the sulfatase family. *Structure 9*, 483−491.
(45) Bond, C. S., Clements, P. R., Ashby, S. J., Collyer, C. A., Harrop, S. J., Hopwood, J. J., and Guss, J. M. (1997) Structure of a human lysosomal sulfatase. *Structure 5*, 277−289.
(46) Hernandez-Guzman, F. G., Higashiyama, T., Pangborn, W., Osawa, Y., and Ghosh, D. (2003) Structure of human estrone sulfatase suggests functional roles of membrane association. *J. Biol. Chem. 278*, 22989−22997.
(47) Lukatela, G., Krauss, N., Theis, K., Selmer, T., Gieselmann, V., von Figura, K., and Saenger, W. (1998) Crystal structure of human arylsulfatase A: the aldehyde function and the metal ion at the active site suggest a novel mechanism for sulfate ester hydrolysis. *Biochemistry 37*, 3654−3664.
(48) Rivera-Colon, Y., Schutsky, E. K., Kita, A. Z., and Garman, S. C. (2012) The Structure of Human GALNS Reveals the Molecular Basis for Mucopolysaccharidosis IV A. *J. Mol. Biol. 423*, 736−751.
(49) Waldow, A., Schmidt, B., Dierks, T., von Bulow, R., and von Figura, K. (1999) Amino acid residues forming the active site of arylsulfatase A. Role in catalytic activity and substrate binding. *J. Biol. Chem. 274*, 12284−12288.
(50) Jonas, S., van Loo, B., Hyvonen, M., and Hollfelder, F. (2008) A new member of the alkaline phosphatase superfamily with a formylglycine nucleophile: structural and kinetic characterisation of a phosphonate monoester hydrolase/phosphodiesterase from *Rhizobium leguminosarum*. *J. Mol. Biol. 384*, 120−136.
(51) Brandao, T. A., Hengge, A. C., and Johnson, S. J. (2010) Insights into the reaction of protein-tyrosine phosphatase 1B: crystal structures for transition state analogs of both catalytic steps. *J. Biol. Chem. 285*, 15874−15883.
(52) Hengge, A. C., Denu, J. M., and Dixon, J. E. (1996) Transition-state structures for the native dual-specific phosphatase VHR and D92N and S131A mutants. Contributions to the driving force for catalysis. *Biochemistry 35*, 7084−7092.
(53) Hengge, A. C., Edens, W. A., and Elsing, H. (1994) Transition-State Structures for Phosphoryl-Transfer Reactions of *p*-Nitrophenyl Phosphate. *J. Am. Chem. Soc. 116*, 5045−5049.
(54) Hengge, A. C., Sowa, G. A., Wu, L., and Zhang, Z. Y. (1995) Nature of the transition state of the protein-tyrosine phosphatase-catalyzed reaction. *Biochemistry 34*, 13982−13987.
(55) Hengge, A. C., Zhao, Y., Wu, L., and Zhang, Z. Y. (1997) Examination of the transition state of the low-molecular mass small tyrosine phosphatase 1. Comparisons with other protein phosphatases. *Biochemistry 36*, 7928−7936.
(56) Keng, Y. F., Wu, L., and Zhang, Z. Y. (1999) Probing the function of the conserved tryptophan in the flexible loop of the *Yersinia* protein-tyrosine phosphatase. *Eur. J. Biochem. 259*, 809−814.
(57) McCain, D. F., Catrina, I. E., Hengge, A. C., and Zhang, Z. Y. (2002) The catalytic mechanism of Cdc25A phosphatase. *J. Biol. Chem. 277*, 11190−11200.
(58) McWhirter, C., Lund, E. A., Tanifum, E. A., Feng, G., Sheikh, Q. I., Hengge, A. C., and Williams, N. H. (2008) Mechanistic study of protein phosphatase-1 (PP1), a catalytically promiscuous enzyme. *J. Am. Chem. Soc. 130*, 13673−13682.
(59) Zhang, Y. L., Hollfelder, F., Gordon, S. J., Chen, L., Keng, Y. F., Wu, L., Herschlag, D., and Zhang, Z. Y. (1999) Impaired transition state complementarity in the hydrolysis of *O*-arylphosphorothioates by protein-tyrosine phosphatases. *Biochemistry 38*, 12111−12123.
(60) Williams, S. J., Denehy, E., and Krenske, E. H. (2014) Experimental and theoretical insights into the mechanisms of sulfate and sulfamate ester hydrolysis and the end products of type I sulfatase inactivation by aryl sulfamates. *J. Org. Chem. 79*, 1995−2005.
(61) O'Brien, P. J., and Herschlag, D. (1999) Catalytic promiscuity and the evolution of new enzymatic activities. *Chem. Biol. 6*, R91−R105.
(62) Khersonsky, O., and Tawfik, D. S. (2010) Enzyme promiscuity: a mechanistic and evolutionary perspective. *Annu. Rev. Biochem. 79*, 471−505.
(63) Babtie, A. C., Bandyopadhyay, S., Olguin, L. F., and Hollfelder, F. (2009) Efficient catalytic promiscuity for chemically distinct reactions. *Angew. Chem., Int. Ed. 48*, 3692−3694.
(64) Mohamed, M. F., and Hollfelder, F. (2013) Efficient, crosswise catalytic promiscuity among enzymes that catalyze phosphoryl transfer. *Biochim. Biophys. Acta, Proteins Proteomics 1834*, 417−424.
(65) Jonas, S., and Hollfelder, F. (2009) Mapping catalytic promiscuity in the alkaline phosphatase superfamily. *Pure Appl. Chem. 81*, 731−742.
(66) Jensen, R. A. (1976) Enzyme recruitment in evolution of new function. *Annu. Rev. Microbiol. 30*, 409−425.
(67) O'Brien, P. J., and Herschlag, D. (1998) Sulfatase Activity of *E. coli* Alkaline Phosphatase Demonstrates a Functional Link to Arylsulfatases, an Evolutionary Related Enzyme Family. *J. Am. Chem. Soc. 120*, 12369−12370.
(68) Miton, C. M., Jonas, S., Fischer, G., Duarte, F., Mohamed, M. F., van Loo, B., Kintses, B., Kamerlin, S. C. L., Tokuriki, N., Hyvonen, M., and Hollfelder, F. (2018) Evolutionary repurposing of a sulfatase: A new Michaelis complex leads to efficient transition state charge offset. *Proc. Natl. Acad. Sci. U. S. A. 115*, E7293−E7302.
(69) Bielicki, J., Fuller, M., Guo, X. H., Morris, C. P., Hopewood, J. J., and Anson, D. S. (1995) Expression, purification and characterization of recombinant human *N*-acetylgalactosamine-6-sulphatase. *Biochem. J. 311*, 333−339.
(70) Bielicki, J., and Hopwood, J. J. (1991) Human liver *N*-acetylgalactosamine 6-sulphatase. Purification and characterization. *Biochem. J. 279*, 515−520.
(71) Kintses, B., Hein, C., Mohamed, M. F., Fischlechner, M., Courtois, F., Laine, C., and Hollfelder, F. (2012) Picoliter cell lysate assays in microfluidic droplet compartments for directed enzyme evolution. *Chem. Biol. 19*, 1001−1009.
(72) Lassila, J. K., Zalatan, J. G., and Herschlag, D. (2011) Biological phosphoryl-transfer reactions: understanding mechanism and catalysis. *Annu. Rev. Biochem. 80*, 669−702.
(73) Beil, S., Kehrli, H., James, P., Staudenmann, W., Cook, A. M., Leisinger, T., and Kertesz, M. A. (1995) Purification and characterization of the arylsulfatase synthesized by *Pseudomonas aeruginosa* PAO during growth in sulfate-free medium and cloning of the arylsulfatase gene (*atsA*). *Eur. J. Biochem. 229*, 385−394.
(74) Hummerjohann, J., Laudenbach, S., Retey, J., Leisinger, T., and Kertesz, M. A. (2000) The sulfur-regulated arylsulfatase gene cluster of *Pseudomonas aeruginosa*, a new member of the *cys* regulon. *J. Bacteriol. 182*, 2055−2058.
(75) von Bülow, R., Schmidt, B., Dierks, T., von Figura, K., and Uson, I. (2001) Crystal structure of an enzyme-substrate complex provides insight into the interaction between human arylsulfatase A and its substrates during catalysis. *J. Mol. Biol. 305*, 269−277.
(76) Appel, M. J., and Bertozzi, C. R. (2015) Formylglycine, a post-translationally generated residue with unique catalytic capabilities and biotechnology applications. *ACS Chem. Biol. 10*, 72−84.
(77) Benkovic, S. J., and Benkovic, P. A. (1966) Studies on Sulfate Esters. I. Nucleophilic Reactions of Amines with *p*-Nitrophenyl Sulfate. *J. Am. Chem. Soc. 88*, 5504−5511.
(78) Hoff, R. H., Larsen, P., and Hengge, A. C. (2001) Isotope effects and medium effects on sulfuryl transfer reactions. *J. Am. Chem. Soc. 123*, 9338−9344.
(79) Dierks, T., Miech, C., Hummerjohann, J., Schmidt, B., Kertesz, M. A., and von Figura, K. (1998) Posttranslational formation of formylglycine in prokaryotic sulfatases by modification of either cysteine or serine. *J. Biol. Chem. 273*, 25560−25564.
(80) Hengge, A. C. (2002) Isotope effects in the study of phosphoryl and sulfuryl transfer reactions. *Acc. Chem. Res. 35*, 105−112.

DOI: 10.1021/acs.biochem.8b00996
Biochemistry 2019, 58, 1363−1378

(81) Admiraal, S. J., and Herschlag, D. (1995) Mapping the transition state for ATP hydrolysis: implications for enzymatic catalysis. *Chem. Biol. 2*, 729−739.
(82) Kirby, A. J., and Varvoglis, A. G. (1967) The Reactivity of Phosphate Esters. Monoester Hydrolysis. *J. Am. Chem. Soc. 89*, 415−423.
(83) Labow, B. I., Herschlag, D., and Jencks, W. P. (1993) Catalysis of the hydrolysis of phosphorylated pyridines by alkaline phosphatase has little or no dependence on the pK_a of the leaving group. *Biochemistry 32*, 8737−8741.
(84) Chapman, E., Bryan, M. C., and Wong, C. H. (2003) Mechanistic studies of β-arylsulfotransferase IV. *Proc. Natl. Acad. Sci. U. S. A. 100*, 910−915.
(85) Chapman, E., Best, M. D., Hanson, S. R., and Wong, C. H. (2004) Sulfotransferases: structure, mechanism, biological activity, inhibition, and synthetic utility. *Angew. Chem., Int. Ed. 43*, 3526−3548.
(86) Hopkins, A., Day, R. A., and Williams, A. (1983) Sulfate Group Transfer between Nitrogen and Oxygen: Evidence Consistent with an Open "Exploded" Transition State. *J. Am. Chem. Soc. 105*, 6062−6070.
(87) Benkovic, S. J., Vergara, E. V., and Hevey, R. C. (1971) Purification and properties of an arylsulfatase from *Aspergillus oryzae*. *J. Biol. Chem. 246*, 4926−4933.
(88) Dodgson, K. S., Spencer, B., and Williams, K. (1956) Studies on sulphatases. 13. The hydrolysis of substituted phenyl sulphates by the arylsulphatase of *Alcaligenes metalcaligenes*. *Biochem. J. 64*, 216−221.
(89) Zalatan, J. G., Fenn, T. D., Brunger, A. T., and Herschlag, D. (2006) Structural and functional comparisons of nucleotide pyrophosphatase/phosphodiesterase and alkaline phosphatase: implications for mechanism and evolution. *Biochemistry 45*, 9788−9803.
(90) Fendler, E. J., and Fendler, J. H. (1968) Hydrolysis of Nitrophenyl and Dinitrophenyl Sulfate Esters. *J. Org. Chem. 33*, 3852−3859.
(91) Kirby, A. J., and Jencks, W. P. (1965) The Reactivity of Nucleophilic Reagents toward the *p*-Nitrophenyl Phosphate Dianion. *J. Am. Chem. Soc. 87*, 3209−3216.
(92) Herschlag, D., and Jencks, W. P. (1989) Phosphoryl Transfer to Anionic Oxygen Nucleophiles. Nature of the Transition State and Electrostatic Repulsion. *J. Am. Chem. Soc. 111*, 7587−7596.
(93) Anslyn, E. V., and Dougherty, D. A. (2006) *Modern Physical Organic Chemistry*, University Science Books, United States.
(94) Cleland, W. W. (2006) Enzyme Mechanisms from Isotope Effects. In *Isotope Effects in Chemistry and Biology*, (Kohen, A., and Limbach, H.-H., Eds.), pp 915−930, CRC Press, Boca Raton, FL.
(95) Hengge, A. C. (2001) Isotope effects in the study of enzymatic phosphoryl transfer reactions. *FEBS Lett. 501*, 99−102.
(96) Hengge, A. C., and Cleland, W. W. (1990) Direct measurement of transition-state bond cleavage in hydrolysis of phosphate esters of *p*-nitrophenol. *J. Am. Chem. Soc. 112*, 7421−7422.
(97) Kuznetsov, V. I., and Hengge, A. C. (2013) New Functional Aspects of the Atypical Protein Tyrosine Phosphatase VHZ. *Biochemistry 52*, 8012−8025.
(98) Hanson, S. R., Best, M. D., and Wong, C. H. (2004) Sulfatases: structure, mechanism, biological activity, inhibition, and synthetic utility. *Angew. Chem., Int. Ed. 43*, 5736−5763.
(99) Kraut, D. A., Carroll, K. S., and Herschlag, D. (2003) Challenges in enzyme mechanism and energetics. *Annu. Rev. Biochem. 72*, 517−571.
(100) Bobyr, E., Lassila, J. K., Wiersma-Koch, H. I., Fenn, T. D., Lee, J. J., Nikolic-Hughes, I., Hodgson, K. O., Rees, D. C., Hedman, B., and Herschlag, D. (2012) High-resolution analysis of Zn^{2+} coordination in the alkaline phosphatase superfamily by EXAFS and x-ray crystallography. *J. Mol. Biol. 415*, 102−117.
(101) Sengerova, B., Tomlinson, C., Atack, J. M., Williams, R., Sayers, J. R., Williams, N. H., and Grasby, J. A. (2010) Bronsted analysis and rate-limiting steps for the T5 flap endonuclease catalyzed hydrolysis of exonucleolytic substrates. *Biochemistry 49*, 8085−8093.
(102) Northrop, D. (1981) The expression of isotope effects on enzyme-catalyzed reactions. *Annu. Rev. Biochem. 50*, 103−131.
(103) Kamerlin, S. C. (2011) Theoretical comparison of *p*-nitrophenyl phosphate and sulfate hydrolysis in aqueous solution: implications for enzyme-catalyzed sulfuryl transfer. *J. Org. Chem. 76*, 9228−9238.
(104) Jencks, W. P. (1969) *Catalysis in Chemistry and Enzymology*, McGraw-Hill, New York, NY.
(105) Williams, A. (2003) *Free Energy Relationships in Organic and Bio-Organic Chemistry*, Royal Society of Chemistry.

DOI: 10.1021/acs.biochem.8b00996
Biochemistry 2019, 58, 1363−1378